



Conférence Européenne  
des Directeurs des Routes  
Conference of European  
Directors of Roads

***AMSTree***

## **CEDR TRANSNATIONAL ROAD RESEARCH PROGRAMME**

### **D3.1 Report outlining current assessment techniques and identifying opportunities how to incorporate new data streams in condition assessment.**

September 2020

---

## Table of contents

1	Introduction .....	5
2	Assessment of Bridges.....	6
2.1	Introduction .....	6
2.2	Type, Frequency and Accuracy of Inspection.....	6
3	Assessment of Roads .....	9
3.1	Introduction .....	9
3.2	Current Assessment Techniques.....	9
4	Techniques for Measuring Damage.....	11
5	New technologies and examples of their application .....	28
5.1	Introduction .....	28
5.2	Laser Scanning and UAV Photogrammetry .....	28
5.3	InSAR .....	32
5.4	UMVs for the detection of Scour.....	34
5.5	Data fusion.....	36
6	Conclusions.....	38
7	Bibliography .....	39

---

## Table of figures

<b>Figure 1:</b> Survey results on a bridge in (a) poor condition and (b) good condition,.....	8
<b>Figure 2</b> a) Traffic Speed Deflectometer (TSD) vehicle and b) the layout of its lasers, after Wright et al. 2016) .....	9
<b>Figure 3</b> Rainfall induced landslide inundates road at Jølster, Norway .....	13
<b>Figure 4</b> Relationship between between soil water content, dielectric constant and propagation velocity of radar waves in unsaturated sands .....	14
<b>Figure 5</b> 3D image of ERT profiles measured by Donohue et al. (2011) .....	15
<b>Figure 6</b> Resistivity Profile in Cross Section Donohue et al. (2011).....	15
<b>Figure 7</b> Composite resistivity and MASW profile along track section .....	16
<b>Figure 8</b> Phases of reflected waves from objects (a) in phase for cavities and (b) out of phase for metallic pipes.....	17
<b>Figure 9</b> Impact echo test (after www.NDT.net) .....	17
<b>Figure 10</b> Simplified concept of an acoustic emission monitoring system deployed .....	19
<b>Figure 11</b> AE rates in response to rainfall events, after Codeglia et al. (2017).....	19
<b>Figure 12</b> a) Location of embedded sensors b) IFSTTAR accelerated pavement testing facility after Bahrani et al. (2020) .....	20
<b>Figure 13</b> Comparison of pavement deflection between deflectometer, geophone and accelerometer a) velocity 8 m/s b) velocity 20 m/s after Bahrani et al. (2020) .....	21
<b>Figure 14</b> Vision-based defect detection vehicle (after Lekshmipathy et al. 2020) .....	21
<b>Figure 15</b> Collapse of Broadmeadow Estuary Bridge Dublin August 2009 .....	22
<b>Figure 16</b> Scour monitoring instrumentation (after Prendergast and Gavin 2013) .....	23
<b>Figure 17</b> Impact of scour on the stiffness of soil .....	24
<b>Figure 18</b> a) Field test b) Numerical model .....	25
<b>Figure 19</b> Comparison of measured frequency with estimate from a numerical model.....	26
<b>Figure 20</b> Elevation of the maximum scour levels as shown in the dive inspection report and in sonar imagery (from Kariyawasam et al. 2019) .....	26
<b>Figure 21</b> Sensor positions on Baildon bridge (from Kariyawasam et al. 2019).....	27
<b>Figure 22</b> Mean PSD of vibrations measured on the South Pier of Baildon bridge during scour-hole filling, (from Kariyawasam et al. 2019) .....	27
<b>Figure 23</b> Development of historic arch bridge models after Armesto et al. (2010) .....	28
<b>Figure 24</b> 3D Models of Kallkallevagen bridge – showing different levels of detail obtained between TLS, CRP and IS (from Poposecu et al. (2019) .....	29
<b>Figure 25</b> CRP Models of Pahtajokk bridge developed using Model 1, 2 and 3 .....	30
<b>Figure 26</b> Workflow to convert point cloud data to carriageway model (Solain et al. (2020) .....	30
<b>Figure 27</b> Methodology for detecting damage from point cloud data and incorporation as semantically rich data in BIM model of bridge (Isailović et al. 2020).....	31
<b>Figure 28</b> IFC structure for geometric representation of damage (Isailović et al. 2020) .....	32
<b>Figure 29</b> The Morandi bridge pre-collapse showing the three A-Frame piers .....	33

<b>Figure 30</b> Time-series deformations on Piers 9,10 and 11 based on CSK/Sentinel 1 A/B satellites from Mililli et al. (2019) .....	34
<b>Figure 31</b> a) Test site at Rollover Pass bridge in the US, b) The Sea-RAI UMV used in survey and c) Results showing no-scour at remaining bridge piers .....	35
<b>Figure 32</b> Multi-beam sonar survey with marine laser structural overlay (Clubley et al. 2015) .....	35
<b>Figure 33</b> Novel spurces of data to provide input for bridge decision support systems .....	36
<b>Figure 34</b> Data fusion of InSAR and GPR to locate and investigate subsidence on an Italian Rail line (Ciampoli et al. 2020) .....	37

# 1 Introduction

Whilst decision-making frameworks used by infrastructure owners are very well developed, a fundamental problem remains that the hazard assessment, which is at the heart of the process is over-reliant on visual inspection. This means that the result is purely qualitative and as a result highly subjective. This leaves the system vulnerable to extreme events and unprepared for future challenges. The inspection is a periodical condition assessment of an asset. Roughly, it is implemented at three levels: (i) Routine inspection (visual examination, performed at fixed time intervals), (ii) Principal inspection (in-depth examination including non-destructive and destructive test methods, performed once every five or six years) and (iii) Special inspection (this includes non-standard testing and is performed in the case where some deterioration is identified e.g. corrosion, scour, settlement etc.). A number of innovations, e.g. in the application of drones, deployment of sensors and automatic high-speed scanning of pavements/structures are currently being developed by road owners.

One of the aims of this project is to establish a framework to integrate this new knowledge into IAMS in order to exploit innovations in inspection and monitoring capabilities. The modern contemporary digital acquisition techniques (e.g. photogrammetry, laser scanning, etc.) need to enhance and improve and be complementary to the qualitative condition assessment currently undertaken. In addition to the benefits of digitizing inspections, the structural health of an asset can be monitored through sensor systems. This provides the potential for assets like bridges and tunnels to become intelligent objects capable of transmitting real-life updates on their condition.

In this project we will follow the definition of terms adopted in Cost Action TU1406 (Hajdin et al. 2018) where:

An **Indicator** is something that describes the state or condition of an object or component (e.g. pavement, bearing, foundation). The indicator can be qualitative (e.g. bad, good, etc.) or quantitative and is based on analysis of one or several observations.

A **Performance indicator (PI)** for road infrastructure is a representation of the fitness for purpose of a physical object such as bridge or its elements. Since the fitness for purpose (i.e. quality) can change over time, so does the value of a performance indicator.

In practice there is no clear distinction between PIs and **Key Performance Indicators (KPIs)**. In this AMSFree project the KPIs relate to a whole bridge, or pavement structure and are as follows:

- 1 Reliability is the probability that an object (bridge or pavement) will be fit for purpose during its service life. It is the complement to the probability of structural failure (safety), operational failure (serviceability) or any other failure mode.
- 2 Availability is the proportion of time the object is open to traffic.
- 3 Safety is the situation of life and limb being protected from harm during the service life of a bridge or pavement. Loss of life and limb due to structural failure is not included by this definition (since it would overlap with the Reliability).
- 4 Economy is related to minimizing the long-term cost of maintenance activities over the service life of a bridge.
- 5 Environment is related to minimizing the harm to environment during the service life of an object.

The overall objective of this deliverable is to identify methods (measurement techniques) that will allow asset managers to obtain quantifiable data to populate the management frameworks.

## **2 Assessment of Bridges**

### **2.1 Introduction**

There are a number of challenges facing asset managers regarding bridge management. The bridge stock in the EU is ageing and subjected to higher loads, faster speeds and extreme weather impacts such as floods. The latter in particular can lead to sudden change of condition. In addition to these issues there is a lack of qualified bridge inspectors to perform onsite safety assessments. As a result, our understanding of resilience across vast networks is uncertain. Where critical events such as collapse occur, the primary focus of infrastructure managers on the safety of road users and workers. However, additional costs of a sudden collapse include the direct costs of repair and the indirect costs, that include traffic disruption, concessionaire penalties, enquiries etc. These additional costs can be up to 10 times higher than the rebuilding costs, Thornes et al. (2012).

Many bridge asset management systems are used across Europe including; BaTMan in Sweden (Safi et al 2013), BAUT in Austria, the Danish Danbro and the German SIB Bauwerke. The principle types of damage affecting bridges are: corrosion of the reinforcement of concrete bridges, and of the structural members in metallic, defects on bearings and expansion joints, concrete spalling, cracks, corrosion of tendons and scour.

### **2.2 Type, Frequency and Accuracy of Inspection**

Prior to any inspection the person tasked with performing the inspection should review the structural systems, the records of maintenance and principal hazards affecting the structure, this is particularly important with regard to legacy structures.

The periodical inspection of an asset comprises:

- (i) Routine inspection (visual examination, performed at a frequency agreed with the overseeing authority (typically once every two years for road bridges). In addition to the structure itself a visual inspection of the adjacent earthworks and waterways should be performed in particular for evidence of scour
- (ii) Principal inspection (in-depth examination, within touching distance including non-destructive and destructive test methods, performed once every five or six years). Again, the inspection should consider the adjacent earthworks and waterways where these might affect the stability of the structure, and
- (iii) Special inspection (this includes weekly or monthly walkovers to observe the development of deterioration or non-standard testing and is performed in the case where some deterioration is identified e.g. corrosion, scour, settlement etc.). In addition (DMRB2017) recommends special investigations are performed in a number of defined situations, including; (a) every six months for cast iron structures and structures with weight restrictions, (b) if an abnormal load will pass over the structure and (c) following the occurrence of natural or man-made hazards. Indeed, the deployment of quick-scan techniques following hazards is an area of growing interest amongst infrastructure managers and governments.

**Table 1** Records obtained from inspections:

Inspection Level	Records
General	Records shall include the condition of all of the elements inspected. Any defects should be identified by type, location and severity in accordance with the asset management system employed by the owner.
Principal	Records shall include: <ul style="list-style-type: none"> <li>(i) condition of all of the elements inspected. Any defects should be identified by type, location and severity in accordance with the asset management system employed by the owner. Where appropriate, photographs and/or sketches of the defects should be included.</li> <li>(ii) Information on significant works performed since the last principal inspection</li> <li>(iii) For bridges over roads headroom measurements should be made</li> <li>(iv) A description of the testing performed as part of the inspection, results and interpretation thereof.</li> </ul>
Special	Records shall include: <ul style="list-style-type: none"> <li>(i) The reason for the inspection</li> <li>(ii) The condition of the element inspected, including photos and sketches</li> <li>(iii) For bridge strikes, details of the vehicle and clearance at point struck.</li> <li>(iv) A description of the testing performed as part of the inspection, results and interpretation thereof.</li> </ul>

Phares et al. (2004) investigated the accuracy and reliability of routine highway bridge inspection condition documentation from the United States in the context of the belief that since they are predominantly based on visual inspection and are thus subjective assessments made by bridge inspectors. Since routine inspection is the most common form of highway bridge inspection in their paper, they compared the results from 49 inspector reports on the condition of the superstructure, substructure and deck of seven case-study bridges. In the rating system applied 0 represents failure whilst 9 represents excellent condition. Comparing the results for two bridges, one where all components (superstructure, substructure and deck) were known to be in poor condition with a reference condition rating of 4, See **Figure 1a** with a bridge where all components were in good condition, reference rating 7, Figure 1b they found;

- a) For the bridge with a known poor condition the average of all 49 inspector's ratings was between 4.3 and 4.9 for the three components. However, the standard deviation in the conditions ratings was in the range 0.76 to 0.94 for the three components. This is reflected in the range of ratings, for example for the bridge deck (Figure 1a) the condition rating varied from a minimum of 2 (critical) to a maximum of 7.
- b) For the bridge in known good condition Figure 1b, the average rating for the components was in the range 6.7 to 7.2. The standard deviation for the components was much lower 0.53 to 0.66 and the maximum range for the assessment of the superstructure was between 5 and 8.

The above suggests that uncertainty or subjectivity of the condition rating determined using visual assessments, increases as the condition of the bridge deteriorates. The authors also examined the field inspection notes taken by the 49 inspectors and found significant variability

in the details provided and instances where defects descriptions were omitted. When examining the photographic records of the inspectors, they note that half the inspectors took only four photographs, the photographs generally showed common details that were taken from easily accessible positions and many defects were not photographed.

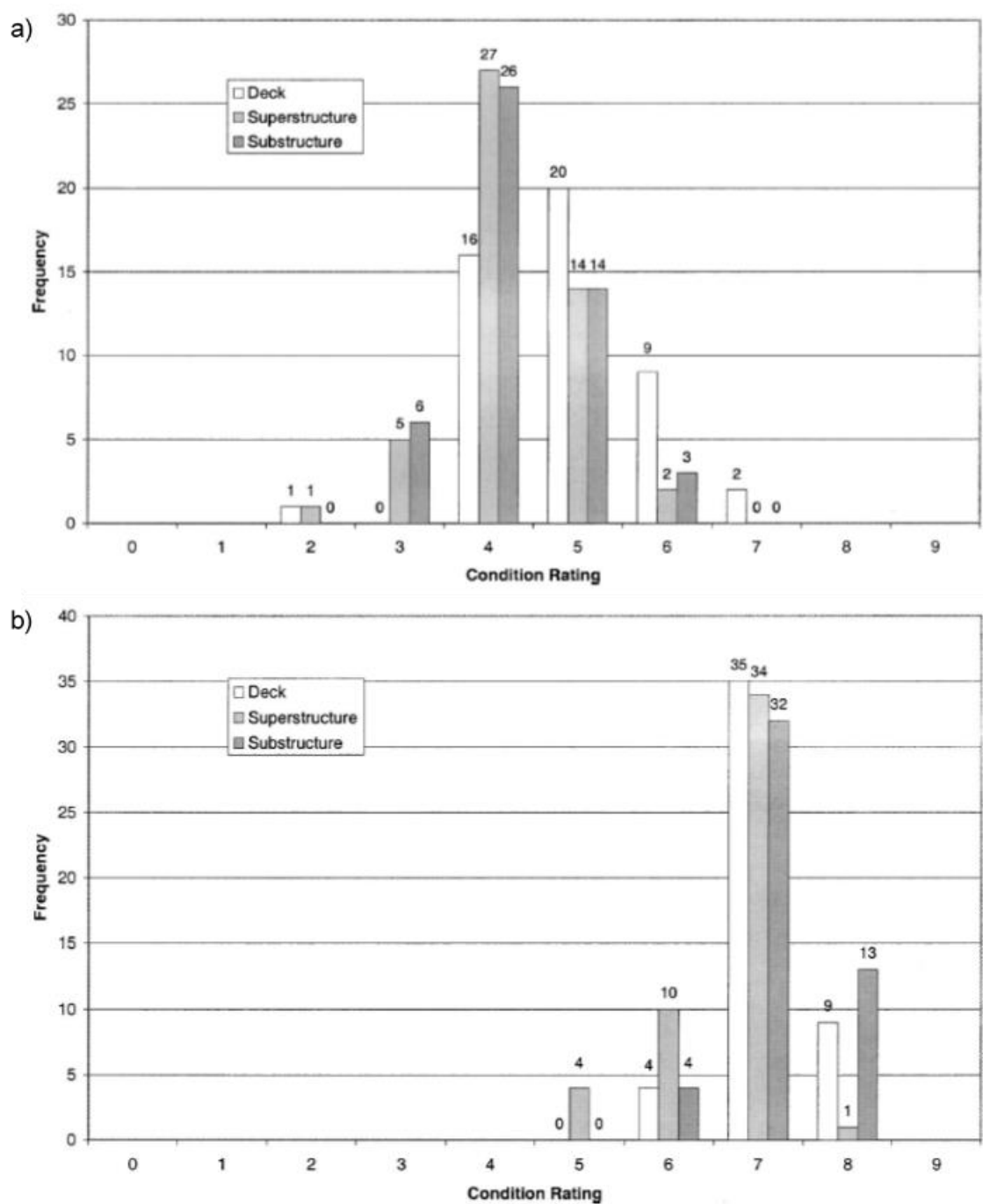


**Figure 1:** Survey results on a bridge in (a) poor condition and (b) good condition, after Phares et al. (2004).



## 3 Assessment of Roads

### 3.1 Introduction

The condition of road pavements affects passenger safety, travel times and comfort in addition to affecting vehicles in terms of emissions, fuel economy and maintenance costs. In recognition of the critical role and impact which road networks have on economic growth and societal health in the EU, road authorities have very well-developed Pavement Management Systems (PMS) that allow resources to be allocated efficiently. Key to the operation of a PMS is accurate information of damage data (Ragnoli et al. 2018). Unlike bridges, the damage detection procedures have largely been automated, See La Torre et al. (2007) and in most cases are applied on moving vehicles. This difference is due to the length of the asset to be evaluated and the necessity not to block traffic flow completely. As with bridges pavement defect categorization varies from country to country, generally the principal defects include; cracking, potholes, surface deformation and miscellaneous distresses (that include lane to shoulder drop-off, water bleeding and pumping (Miller and Bellinger 2014). In addition, during condition assessment pavement quality characteristics are measured.

### 3.2 Current Assessment Techniques

In general conditions assessment consists of measuring (i) Structural condition, (ii) surface unevenness and (iii) skid resistance. The CEDR HiSPEQ project (2013) considered methods including combined use of Traffic Speed Deflectometer (TSD) and GPR to determine the structural condition of the road, see **Figure 2**. Specifically, they recommended that TSD measurements be combined with what they term dynamic information on surface evenness, rutting and cracking information to track deterioration in the road surface. The TSD measures the deflected pavement surface using a series of laser vibrometers, **Figure 2b**. In contrast they suggest since they assume GPR data is used to give the road structure, this can be seen as static data and the frequency of measurement can be reduced.



**Figure 2** a) Traffic Speed Deflectometer (TSD) vehicle and b) the layout of its lasers, after Wright et al. 2016)

Highways England adopt the TRAFFIC-speed Condition Surveys (TRACS) to measure surface condition, Sideway-force Coefficient Routine Investigation Machine (SCRIM) to measure skid resistance and TSD for structural conditions, see Spielhofer et al. (2015). These measurements are supplemented by GPR used to measure pavement thickness. The survey frequency depends on the importance of the road and the part of the road, with the two-main lanes of the strategic road network being monitored annually.

The CEDR Hi-SPEQ project (Wright et al. 2016) reviewed the equipment used to obtain high-speed condition of pavements in order to provide guidance for CEDR members on the operation, quality and specification of these systems. Based on a literature review and owner

survey they note that surface defect evaluation was commonly performed by image evaluations. Image analyses were performed either by a human operator or through some machine learning approach. For measuring the pavement structure and stiffness, the Hi-SPEQ review showed that most road owners used the Falling Weight Deflectometer (FWD) or Lacroix Delflectograph.

Coenen and Golroo (2017) provided a comprehensive review of automated methods for collection of data on pavement distress. In this analysis they differentiate whether the methods had commercial application (C) or were proposed in research papers (P), See **Table 2**.

**Table 2** Common defects and automated methods for detection (adapted from Coenen and Golroo 2017)

Defect	Camera	Accelerometer	Laser	Microphone	Sonar	Pressure
Cracking	C		C			
Potholes	C	C	C	P	P	C
Surface Deformation	P	P	C		C	
Misc. Distress	P		C	C	C	

## 4 Techniques for Measuring Damage

Kusar et al (2019) present an evaluation of NDT methods commonly used for the inspection of concrete, stone and masonry bridges in the EU. The methods were evaluated using six criteria including; test duration, status of standardization of the test procedure, data reliability, diversity of use (e.g. can the test measure more than one type of damage) and complexity of interpretation. The criteria were scored by a group of experts from COST Action TU1406 and an Analytical Hierarchy Process was used to quantify the results and utility functions are determined to rank the methods for use in 3 categories, methods for determining material properties, damage detection and identifying corrosion, See **Table 3**. An interesting finding is that the methods related to measurement of material properties scored high utility functions (with higher scores indicating the best method), despite some of the methods such as the rebound hammer having low reliability. The high utility scores were achieved because the methods were fast, cheap and easy to interpret. Many of the approaches considered for damage detection (including GPR, Acoustic Emission, Thermography and Impact Echo Tests) had lower Utility Functions with the weaknesses identified to be the complexity of interpretation followed by the test duration.

**Table 3** Utility functions determined from a range of damage detection methods after Kusar et al. (2018)

Application	Utility function (out of 3)	NDT method
Material Properties	2.71	Cover measurement
	2.55	Phenolphthalein test
	2.43	Probe penetration test
	2.42	Pull-off test
	2.22	Rebound hammer
Damage and Defects	2.22	Impact echo
	1.86	Thermography
	1.80	Ground Penetrating Radar
	1.63	Ultrasonic pulse echo
Corrosion	1.89	Half-cell potential
	1.82	Galvanostatic pulse
	1.82	Electrical resistivity
	1.65	Linear polarization resistance

Visual inspection and NDT provide snapshots of the condition of an asset assessment whereas Structural Health Monitoring (SHM) is used to continuously monitor some degradation process. In many cases it should be borne in mind that many SHM techniques are developed for a single purpose and provide no data on other potential processes. The specific uses include; Concrete shrinkage, substructure settlement or rotation, cracking and rupture of tendons or cables. In addition, Weigh in Motion (WiM) technologies are designed to determine real load data. One of the main advantages of SHM is that it allows model updating, based on comparison with a computational model validated to the condition at a fixed time (e.g. the start of monitoring). Many reviews of technologies mix SHM methods with those that are used in routine damage detection studies. This is in-part because some of the techniques, e.g. GPR, Acoustic Emission etc. can in-fact be used for both in snap-shot damage assessment and also

in monitoring degradation process, e.g. SHM. In this report we first consider the key techniques of damage detection currently used in condition assessment. (CA) The focus of the AIMS-Free project is on incorporating damage detection data in BIM and therefore this report will consider methods to determine damage directly or indirectly. For comprehensive reviews of methods to determine material properties the reader is referred to comprehensive reviews e.g. NPRA (2005), Gastineau et al. (2009).

**Table 4** Existing techniques for SHM updated after Gastineau et al. (2009)

Method	Classification
GPR	CA and SHM
Accelerometers (new?)	SHM
Acoustic Emission	CA and SHM
Automated laser total station using prisms for displacement	CA and SHM
Resistivity	CA
3D laser scanners	CA and SHM
Electrochemical Fatigue Sensing System	SHM
Electrical Impedance (Post-Tensioning Tendons)	SHM
Fiber optics	SHM
Potential Measurements	CA
Impact echo test	CA
Tomography for void detection	CA

### **Ground Penetrating Radar**

Ground Penetrating Radar (GPR) is a non-destructive method of subsurface imaging using electromagnetic radiation. Electromagnetic waves, or radar pulses, in the range of 10 to 1000hz are transmitted into the subsurface and are reflected from discontinuities, e.g. layer interfaces, voids etc. (Dong and Ansari, 2011). The method can be applied in urban and rural environments and is applicable on all types of road surfaces and paved areas. GPR is an effective tool for mapping foundations, voids/cavities and structural features. Since the frequency adopted for the GPR survey controls two crucial survey parameters – the investigation depth and resolution the use of multiple antennae is common. As a frequency plateau usually occurs in the 1 MHz to 1000 MHz. Higher frequencies provide improved resolution at shallow depths lower frequencies are adopted for deeper investigations, Kovacevic et al. (2017).

Ground Penetrating Radar is routinely used to examine the general deterioration of concrete, particularly in bridge decks by comparing periodic surveys (Parillo 2009 and Yehia 2008). GPR data allows identification of the locations of cracks, voids, delamination, and corrosion with trials showing the method achieve similar accuracy to chain dragging and visual inspection. Furthermore, comparisons of GPR to core samples have also been precise (Parillo 2009, Yehia 2008). GPR is routinely used to map reinforcement in concrete elements with Hugenschmidt and Mastrangelo (2006) demonstrating that a very high frequency (2 GHz) antenna could determine the location and cover depth of reinforcing bars and the pre- and post-tensioning cable trajectories in bridges.

GPR is also useful in the measurement of thickness of asphalt and unbound pavement layer thicknesses for quality control and quality assurance Pitonák and Filipovsky (2016), for determining damaged areas in embankments including ballast fouling, burrows, and the water content of the soil, Kovacevic et al. (2017) and to identify progressive failure due to settlement beneath embankments, Donohue et al. (2011).

Plati and Loizis (2013) applied GPR to determine the in-situ density and moisture content in asphalt pavements. Dong et al. (2016) provided a field validation of the ability of a vehicle-mounted GPR system to detect the thicknesses and defects (including delamination and poor compaction) of asphalt pavements. The addition of GPS and digital cameras allowed the precise location of defects to be determined. The field tests showed that method achieved predicted thickness of the surface layer and top surface layer were less than 3% and 5%. Plati et al. (2020) correlate FWD measurements with GPR to determine the thickness of road pavements.

Landslides present a serious geohazard across the world, causing hundreds of billions of euros in damage and thousands of deaths and injuries annually, Aleotti and Chowdury (1999), Martinovic et al. (2014). One of the areas where landslide consequences are especially high is along the major transportation lines, where landslides are responsible for significant direct and indirect damages including destruction of infrastructure, network disruptions, along with the potential for human casualties, see Figure 3 (Klose et al. 2014). Given the stability of many earthworks, particularly those adjacent to transport networks is dependent on the partial saturation of the soil, See Gavin and Xue (2009, 2010), simple methods to determine the water content of near surface soils and their temporal variation are particularly important for infrastructure owners.



**Figure 3** Rainfall induced landslide inundates road at Jølster, Norway  
(Photo: HRS Sør-Norge)

Since the dielectric constant of granular sediments is dominantly governed by water content Van Overmeeren et al. (1997) presented a relation between soil water content, dielectric constant and propagation velocity of radar waves in unsaturated sands, shown in **Figure 4**.



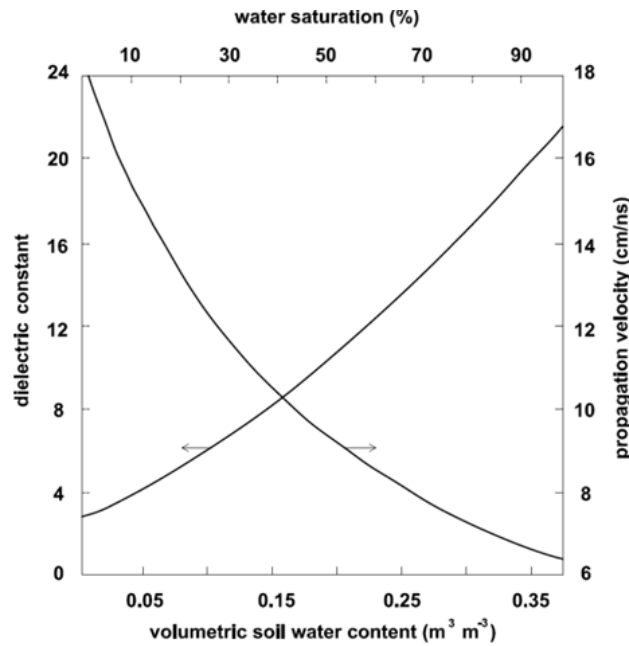


**Figure 4** Relationship between soil water content, dielectric constant and propagation velocity of radar waves in unsaturated sands (Van Overmeeren et al., 1997)

Donohue et al. (2011) performed a GPR survey at the site of a slope failure of a 5m high embankment on the Irish Rail network. The GPR survey identified a deep ballast layer (maximum depth approx. 2m or 40% of the embankment height) near the location of the failure. There was clearly evidence of a long-term settlement problem at this location with maintenance work consisting of frequent ballasting to maintain the track level. The GPR profile along the section showed indication of multiple interfaces in the ballast layer, indicative of repeated tamping. No records of this maintenance activity were maintained as no system existed at that time to hold such information. The deepest ballast layer was identified as a hot-spot (an area which shows an indication of incipient failure). Having identified this location a more comprehensive geophysical investigation was undertaken.

The first method adopted was Electrical resistivity tomography (ERT). ERT is used to calculate the electrical resistivity distribution of the subsurface by measuring a large number of electrical potential differences for different combinations of surface electrodes. A number of authors have used resistivity measurements to investigate landslides and slope stability problems, including determining the soil within the failure surfaces, (Lapenna et al. 2003; Israil and Pachauri 2003; Göktürkler et al. 2008), the location of the shear failure surface (Caris and Van Asch 1991; Godio and Bottino 2001; Göktürkler et al. 2008), landslide hazard assessments for active slides (e.g., Schmutz et al. 2000; Mondal et al. 2008) and investigation of the effects of rainfall infiltration (Caris and Van Asch 1991; Suzuki and Higashi 2001; Friedel et al. 2006).

Two ERT profiles were taken, the first profile (ERT 1) was perpendicular to the embankment, at the centre of the location of the rotational failure zone. The other profiles (ERT 2 and ERT 3) were both located parallel to the traffic direction at the top of the embankment, see **Figure 5** where low resistivity indicates weak soils.

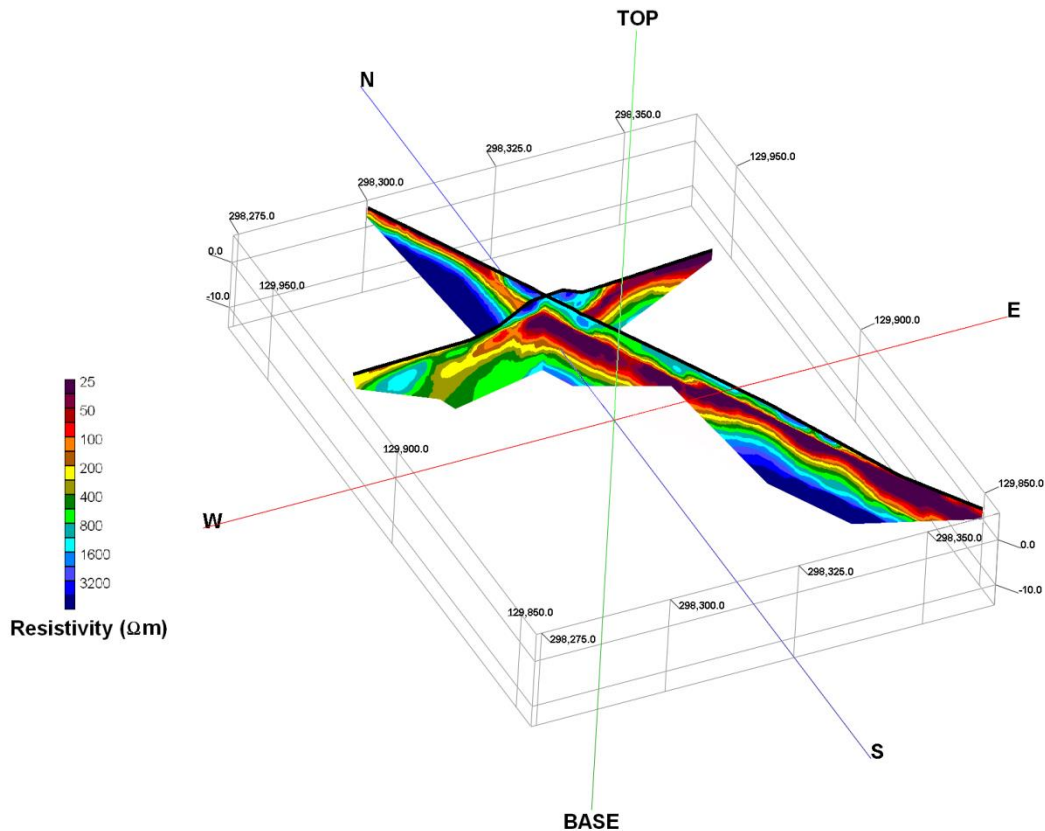


**Figure 5** 3D image of ERT profiles measured by Donohue et al. (2011)

The ERT1 profile across the failure surface indicated the presence of a deep pocket of soft soil (red zone) directly beneath and to the East (right hand side) where the failure occurred, See **Figure 6**.

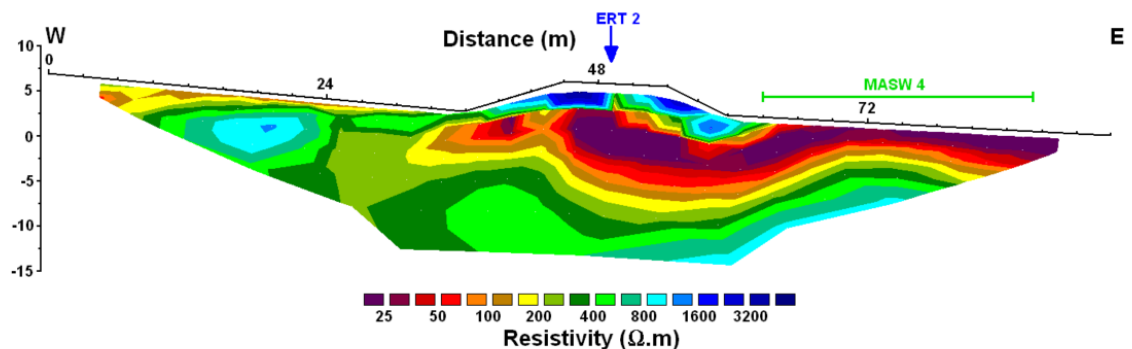


**Figure 6** Resistivity Profile in Cross Section Donohue et al. (2011)

Because of the likely role of this soft layer in stability of the embankment, measurements of the soil stiffness were required for modelling. Multichannel analysis of surface waves (MASW) which utilise surface waves for the estimation of shear-wave velocity ( $V_s$ ) was first introduced in the late 1990s by Park et al. (1999) and Xia et al. (1999). The method is similar to spectral analysis of the surface-waves (SASW) method (Nazarian and Stokoe 1984), the most significant difference between the SASW and the MASW techniques, involves the use of multiple receivers with the MASW method (usually 12– 60 receivers), which increases the speed of the operation. Another advantage of the MASW approach is the ability of the

technique to identify and separate fundamental and higher mode surface waves. According to elastic theory, the small strain shear modulus,  $G_{\max}$ , is related to  $V_s$  by the following equation:

$$[1] \quad G_{\max} = \rho V_s^2$$

Where:  $G_{\max}$  = shear modulus (Pa),  $V_s$  = shear wave velocity (m/s) and  $\rho$  = density (kg/m<sup>3</sup>). The  $V_s$  profiles are combined with the ERT2 and ERT3 profiles in **Figure 7**. The small strain stiffness derived from the data was combined with lab tests to determine creep and strength parameters of the soft soil layers. The location of soil samples for lab testing was directed using the ERT and MASW profiles.

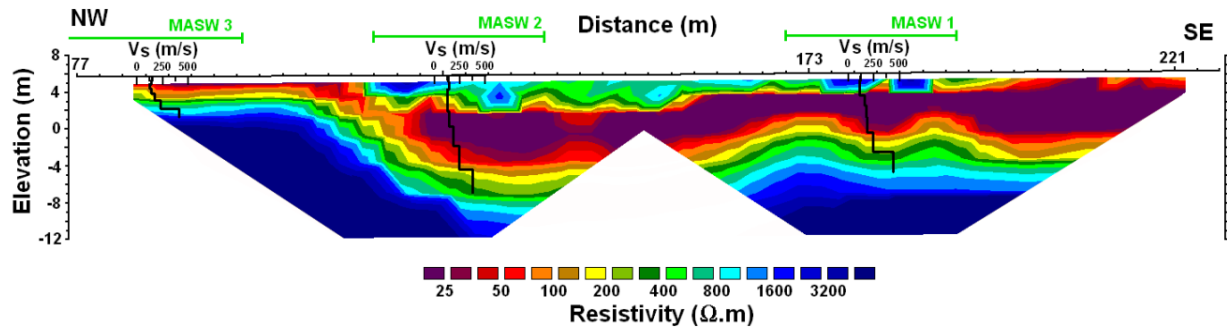


**Figure 7** Composite resistivity and MASW profile along track section

In conclusion the authors note that periodic GPR profiling would have identified the risk of this location to rotation slope failure, even in the absence of proper records of ballast maintenance. The failure that occurred was triggered by inappropriate remediation works as the infrastructure owner attempted to increase the safety of the embankment, without a clear understanding of the mechanisms controlling the ongoing settlement problems at the location.

The relatively simple conversion of shear wave velocity to small strain shear stiffness (or Young's modulus) makes it an ideal tool to provide input for response models and it has been used to derive stiffness profiles for highway pavements (Li et al. 2018) and to determine the mechanisms governing long-term settlement of immersed tube tunnels, Gavin et al. (2020). In addition, as the stiffness of soil is controlled by in-situ stress level (which changes with water content) Donohue et al. (2014) show that periodic MASW surveys are useful in the assessment of climate effects.

One disadvantages of GPR is that the data analysis is complex and subjective. Ciampoli et al. (2019) describe a multi-stage quality assurance procedure that comprises; raw signal correction, removal of low-frequency harmonics and antennae ringing, signal gain and band-pass filtering. Park et al. (2018) considered the problem of object detection in urban roads where signals are often weak and noisy and propose a novel a phase analysis technique to address these weaknesses. The proposed method allows the operator to objectively determine the location and nature of an object. A field test demonstrated the method could locate and identify cavities, pipes and gravel pockets in an urban road environment based on whether a signal is in or out of phase and the phase change ratio. For example, the cavity which has low permittivity has a reflection, in phase with the direct wave, whilst the metallic pipe is out of phase, See **Figure 8**.



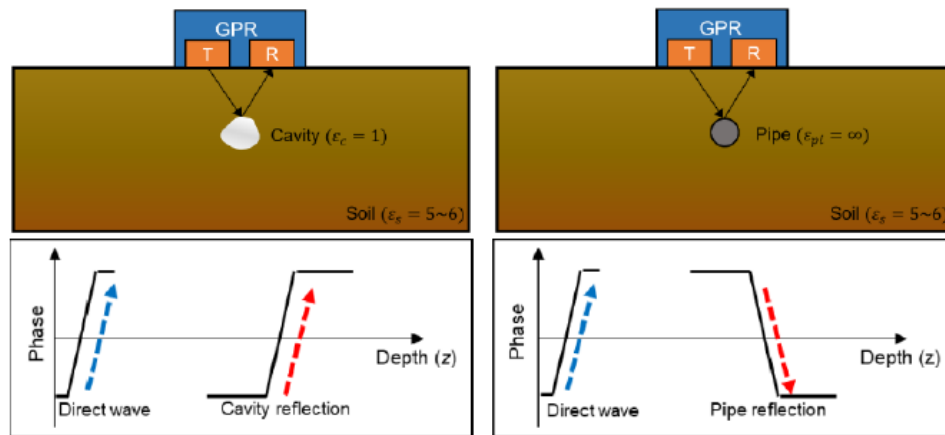


**Figure 8** Phases of reflected waves from objects (a) in phase for cavities and (b) out of phase for metallic pipes

Hugenschmidt (2002) and Anderson et al. (2007) used floating antennae that moved across the surface of the water to show that GPR is a safe and effective way to observe scour near bridges, and the GPR tool does not need to be connected to the river bed. This is particularly useful during peak flooding times, as it allows time for preventative action to be taken (Anderson et al., 2007). Anderson et al. (2007) prove in addition the system is capable of identifying in-fill features. For a comprehensive review of GPR applications in Civil Engineering, See Wai-Lok Lai et al. (2020).

### Impact Echo

The impact-echo method is a non-destructive method for measuring the depth of structural members and concrete road slabs using impact generated stress (Sansalone and Streett, 1998). The surface is struck with a round sphere, and the frequency (Hz) of the response is measured. From this frequency, the depth of the slab can be calculated. If the calculated depth is not equal to the actual depth of the slab this indicates that a defect such as delamination is present (Sansalone 1993) and allows the depth to be calculated (Yehia et al. 2007). The impact-echo method is commonly used on bridge decks to detect abnormalities during routine checks however, it also has applications for flaw detection in highway pavements, buildings, tunnels, piers, dams, seawalls and other structures. The test results also allow three-dimensional maps of a deck to be visualized (Gucunski et al. 2006 and Yehia et al. 2007).

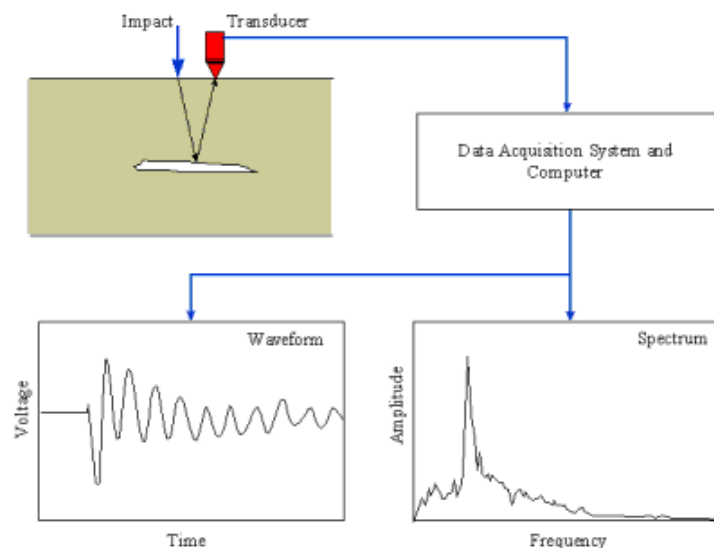


**Figure 9** Impact echo test (after [www.ndt.net](http://www.ndt.net))

The main components of the impact echo system are a cylindrical transducer unit to record surface displacements resulting from the reflections of the waves, spherical impactors which give rise to the low-frequency stress waves that pass into the structure, a portable computer, an analog-to-digital data acquisition system and a software program to control the tests and show the results both graphically and numerically (Sansalone and Streett, 1998). Displacement versus time signals that result become transformed into the frequency domain and plots of amplitude versus frequency, or spectra, are produced. The numerous reflections of stress waves between the impact surface, flaws, and other surfaces result in transient resonances. These transient resonances can be located in the spectrum, and thus aid in pinpointing flaws and determining the integrity of the structure. Azari and Lin (2019) note that asphalt overlays are known to affect the test results and general are to perform tests in cold weather. Based on a laboratory study they recommend the test be performed at temperatures of 32°F and below.

### ***Infrared Thermography***

Infrared Thermography (IRT) is a process in which a thermal imager is used to detect emitted heat from an object, converting it to temperature and generates an image of the distribution of temperature in the object. It can be used as a method of scanning concrete for subsurface flaws, and typically is used for assessing concrete decks. The camera detects infrared radiation and can map its intensity. The emissivity of the surface dictates the intensity of the radiation and variation in intensity indicates subsurface abnormalities in the concrete. Factors causing abnormalities can include spalling due to corrosion and delamination among other things (Maser et al. 1990, MDOT 2009).

Heat exchange between an object and its surroundings involves conduction, convection, and heat radiation can be described as the generation of electromagnetic waves comprising of a range of wavelengths (Cheng et al., 2008). Infrared radiation covers wavelengths from 0.75 to 14  $\mu\text{m}$ , lying between visible and microwave ranges in the electromagnetic spectrum. Infrared thermography is based on the idea the transfer of heat in any given material is impacted by changes in thermal properties of the material, particularly those caused by concealed subsurface anomalies. Infrared cameras can detect and register infrared radiation from surfaces, and differences in temperature on the surface possibly resulting from subsurface defects can be isolated based on the thermal images (Cheng et al., 2008). Hiasa (2016) compared the performance of three different infrared cameras under laboratory conditions and found that although each camera shows different temperature readings, since they captured temperature differences between sound areas and defects. This did not impact their efficacy in detecting damage.

Marchetti et al. (2008) performed laboratory experiments to show the technique could identify damage (laminations) in road structures. Advantages associated with infrared thermography include rapid, easily interpreted results as well as the equipment being portable. Thermography can also be carried out with minimal traffic delays, particularly in comparison to other methods of investigating subsurface structures such as chain dragging (Maser et al. 1990, Yehia et al. 2007). However, they note there are also several drawbacks associated with using infrared thermography, particularly that variation in surface texture and debris can cause changes in intensity. Additionally, if the concrete has been overlaid by asphalt, this can lead to misleading results. Weather conditions and air temperature also need to be considered, as both of these factors affect the radiation emitted from the bridge deck (Maser et al. 1990, Yehia et al. 2007). Furthermore, if water occupies the voids rather than air the voids will not be detectable. Haisa (2016) performed a combination of lab and numerical analyses to determine the optimum period to perform an IRT survey to minimize errors due to ambient temperatures and concluded that surveys should be conducted at nighttime.

## Acoustic Emissions

Acoustic emission (AE) describes the phenomenon of the propagation of sub-audible waves due to permanent changes in a material due to energy release. In soil, many slope failures develop over-time and movements along the frictional shear plane mobilized during soil failure and as a result of rock displacement along existing discontinuities and the generation of new fractures will result in energy release some time before failure. As a result, monitoring of acoustics emissions can provide vital information on incipient failures. In concrete and other man-made materials, the release of stored elastic energy or redistribution of stresses caused by loading, chemical reaction or other potential damage processes can also be recorded.

Codeglia et al. (2017) describe the deployment of an AE based monitoring system for rock falls capable of producing real-time warning of ground movements, See **Figure 10**. A waveguide placed in a borehole secured below the likely failure plane is used to direct AE waves to a piezoelectric transducer mounted above ground level. In soil slopes that generate very low AE levels the borehole is backfilled with gravel or coarse sand which acts a wave generator. A sensor node is used to amplify the signal and filter frequencies below 20 kHz (environmental background noise) and above 30 kHz to preserve battery life. A trigger voltage (between 0.05 and 0.49V) and a sampling frequency (between 1 min and 60 min) is chosen. The number of times the trigger voltage is exceeded in the chosen time periods is compared to four pre-determined alarm levels and a warning status is transmitted by SMS when required.

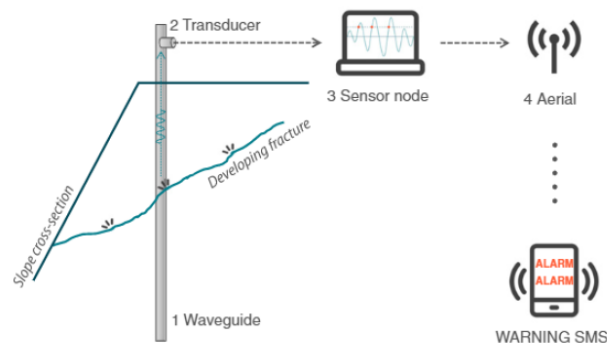


**Figure 10** Simplified concept of an acoustic emission monitoring system deployed in a rock slope, after Codeglia et al. (2017)

The results of monitoring over a 2-week period are shown in **Figure 11**, where it can be seen that AE emissions are strongly correlated with rainfall events.

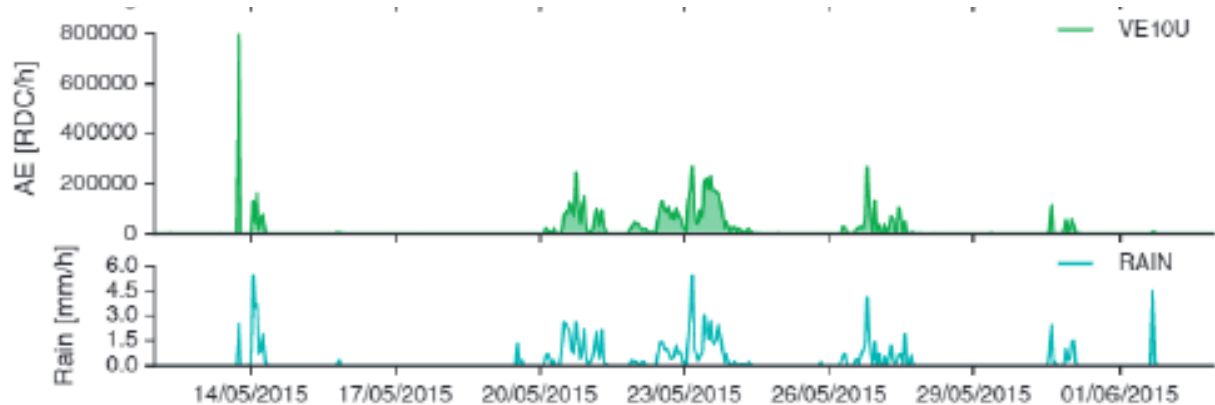


**Figure 11** AE rates in response to rainfall events, after Codeglia et al. (2017)

Worley et al. (2019) describe a lab and factory-based study of the application of AE for crack monitoring in concrete bridge girders. Although AE was a good indicator of crack propagation in both environments and for a range of construction processes including pre- and post-tensioned members, the authors concluded that the technique was not yet at a stage of development to use in quality assurance procedures.

Mednis et al. (2000) used acoustic methods to detect major road surface defects such as bumps and potholes. Kongrattanasert et al. (2010) and Zhang et al. (2013) demonstrated that raveling, bleeding and road smoothness could be detected by microphones placed near the wheel and even alongside the roadway. Fedele et al. (2017) used microphones embedded in a pavement to record vibro-acoustic signals from passing traffic. Analysis of output allowed information about the presence and the severity of cracks to be determined.

### Accelerometers

Accelerometers record acceleration at a given instant allowing and sampling at high frequencies is possible. Following numerical integration, a displacement (or velocity) history can be obtained. They are available as relative low-cost sensors that can be attached to a structure and most modern phones and vehicles also collect acceleration data that could be useful in infrastructure monitoring. Since an uneven road surface and the presence of potholes or other damage in particular creates driving discomfort due to the development of vibrations, accelerometers have long been recognized as a potential form of automatic detection tool. However, such instruments collect a large amount of data and therefore storage and processing are an issue. In addition, errors can be propagated during the numerical integration process suggested by Park (2007) which means a focus on the quality assurance is required.

Bahrani et al. (2020) conducted laboratory and field experiments to test whether accelerometers and or geophones could be used to provide continuous measurement of the deflection of pavements under real traffic loading. Four commercially available sensors were tested, two accelerometers and two geophones that were chosen based on the following specified criteria; (i) low-cost, (ii) durability, (iii) compactness, (iv) resonant frequency lower than 2Hz and sensitivity to deflection measurements between 0.1 and 1mm. As neither system outputs deflection directly, a transformation model is required to obtain pavement deflection. A procedure involving signal filtering, amplification, integration and transformation A laboratory test programme proved that consistent predictions of pavement deflection were obtained using sensors embedded in pavement materials. Follow-on field tests were performed using two accelerometers and two geophones embedded in the IFSTTAR accelerated pavement testing facility, See **Figure 12**.

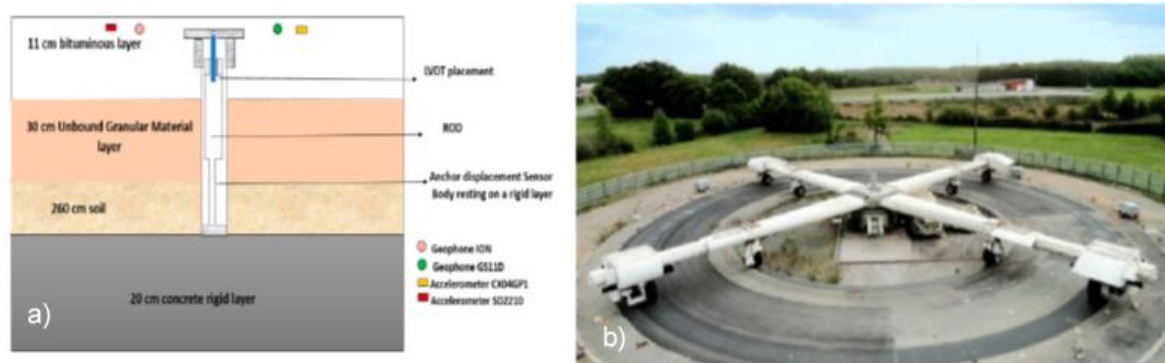


**Figure 12** a) Location of embedded sensors b) IFSTTAR accelerated pavement testing facility after Bahrani et al. (2020)

The test programme explored the effect of vehicle speed and truck weight. The geophones and accelerometers provided deflected shapes that were very close to those recorded by the

reference anchor deflectometer across the range of vehicle speeds considered, see **Figure 13**.

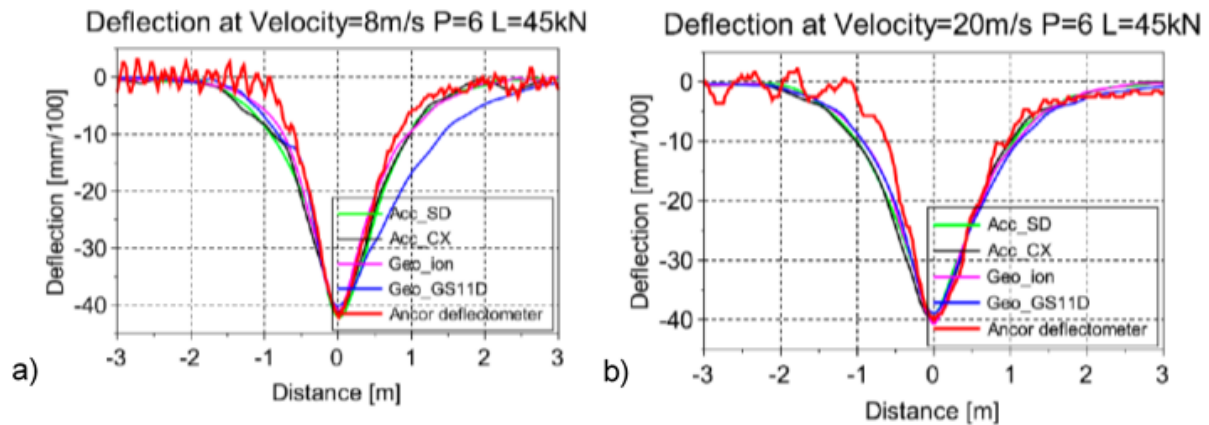


**Figure 13** Comparison of pavement deflection between deflectometer, geophone and accelerometer  
a) velocity 8 m/s b) velocity 20 m/s after Bahrani et al. (2020)

Lekshmipathy et al. (2020) investigated the use of vibration measurements made using a smartphone (collecting accelerometer and gyroscope readings) to detect damage including uneven surface (bumps), cracks and potholes on ten study roads located with the campus of National Institute of Technology Tiruchirappalli campus, India. Prior to this study data was collected from nineteen independent roads, with a study length of approximately 15km to train an Artificial Neural Network (ANN) to detect these defects. In total 5690 readings were used in the training set. For the ten study roads a further training set consisting of 70% of data were used to detect and classify defects and the remaining 30% was used for validation.

The ability to identify defects was compared to a vision-based system. For this part of the study a regular car, with a Sony Handycam of 8.9 MP resolution fixed to the rear, was driven at a speed between 10-15 km/hr. across the test sections.

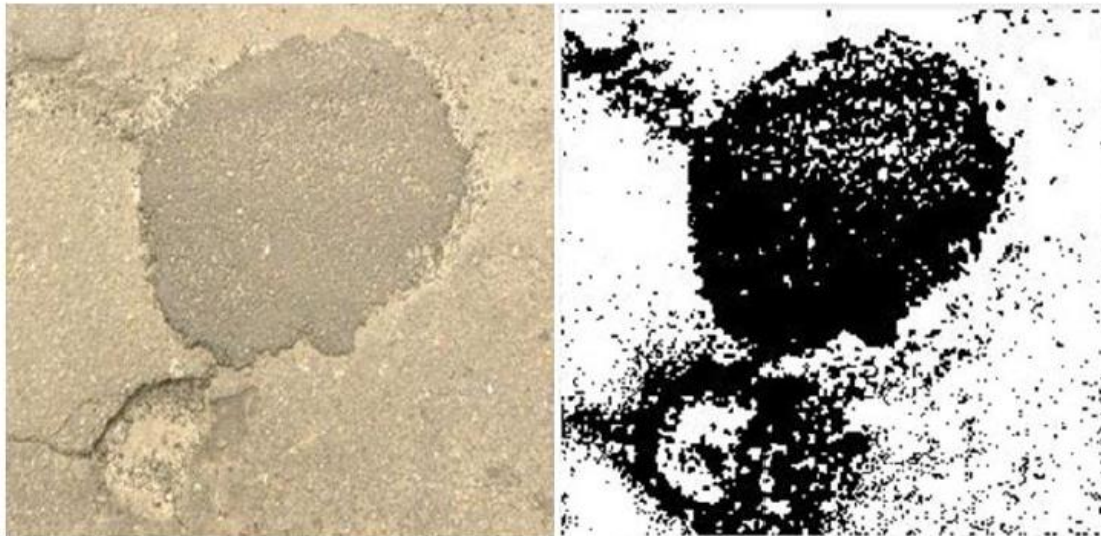


**Figure 14** Vision-based defect detection vehicle (after Lekshmipathy et al. 2020)

The accuracy of the vibration and vision methods was 90% for detecting potholes, see **Figure 14**, the vibration-based methods detected 100% of bumps, whilst the vision method could not detect these. The vision-based method detected 76% of cracks compared to 10% for the vibration-based methods. The authors note that the vision-based method has the disadvantage that post-processing was computationally expensive.



Scour erosion of bridge foundation soil is the number one cause of bridge failure in bridges located over waterways (Forde et al, 1999; Melville & Coleman, 2000; Shirole & Holt, 1991). In the United States, the average cost for flood damage repair of highways is estimated at €42 million per year (Arneson et al. 2012). Scour failures typically occur quite suddenly, with the result that the risk of loss of life is high. **Figure 15** shows the Malahide Viaduct, in North Dublin, Ireland, that failed suddenly as a commuter train passed over it (Maddison, 2012). Fortunately, there were no casualties in this event; however, this section of the TEN-T railway between line between Dublin and Belfast, was closed for several months as a result of the collapse.



**Figure 15** Collapse of Broadmeadow Estuary Bridge Dublin August 2009  
(image courtesy Irish Rail)

Whilst the collapse of the Malahide viaduct was sudden, it was not without warning. The bridge owner was warned of unusual flows around the pier that collapsed in the weeks preceding the failure. In response a visual inspection was conducted, and a measurement train traversed the bridge in the days before it collapsed. Both suggested that the bridge was not in imminent danger. A report by the Railway Accident Investigation Unit (2010) blamed the failure on loss of corporate memory. The investigation revealed that the bridge suffered from scour effects from the time it was first constructed, and a number of significant interventions had been undertaken during the life of the bridge. The investigation revealed that a report prepared in 1997 (12 years before the failure) had highlighted the susceptibility of the bridge to scour and indicated that scour was evident around the pier that eventually collapsed. Unfortunately, this report was not in the Bridge management system and therefore the engineers responsible for the 2009 inspection had no knowledge of the scour issue.

Current visual inspection methods include view from the bank/bridge at times of low water level and the use of divers and basic bathymetric surveys. The use of divers has a number of challenges, work in low visibility, difficult to take measurements, risk means that work occurs outside of flood events and therefore scour holes may have infilled etc.

A number of scour measurement devices have been proposed, See (De Falco & Mele, 2002, Forde et al. 1999 and Gavin et al. 2018). Methodologies developed can be broadly categorized as follows:

- 1 Methods, which directly measure the scour depth using instrumentation, and

- 2 Indirect methods, which infer scour severity by tracking changes in bridge modal properties, e.g., natural frequency.
- 3 Use of drones, UAVs or submersibles

### **Direct methods**

A range of sensors and methods for direct scour monitoring have been developed and are described in Prendergast and Gavin, (2014), See **Figure 16**. The operation of simple systems such as Float-Out Devices and Tethered Buried Switches are described by Briaud et al, (2011) and Hunt, (2009). These simple mechanical devices float out of the soil when scour reaches their installed depth, triggering a signal. However, they must be reset when they float out, thus being maintenance intensive.

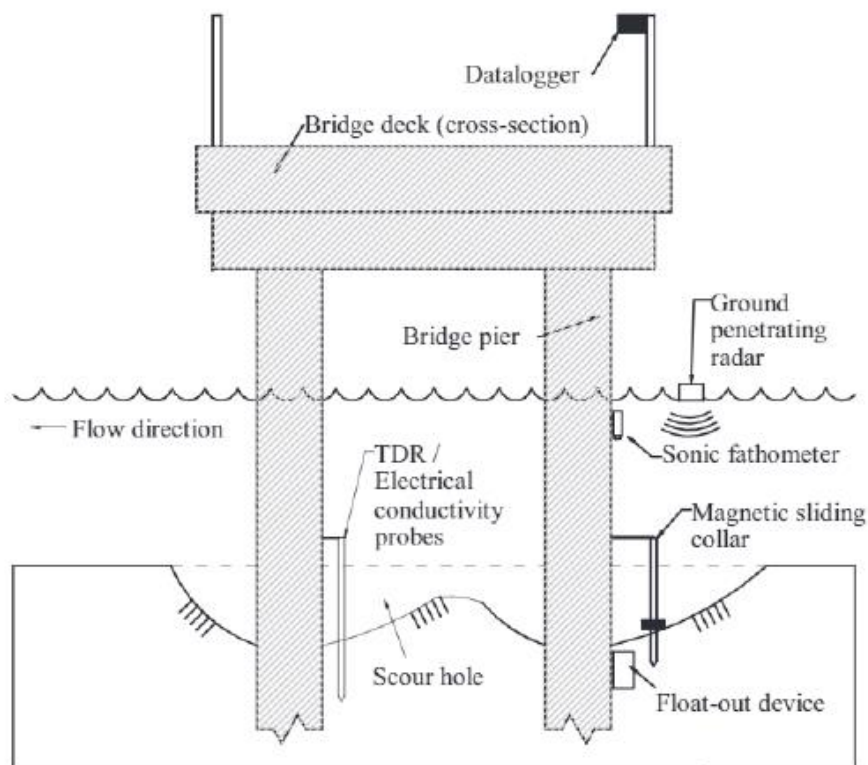


**Figure 16** Scour monitoring instrumentation (after Prendergast and Gavin 2013)

Time-Domain Reflectometry (TDR) systems use changes in dielectric permittivity to monitor the location of the soil-water interface relative to a fixed probe (Fisher et al. 2013; Yu & Yu, 2009). Soundwave devices such as Sonic Fathometers (Fisher et al. 2013; Nassif et al. 2002; Reflection Seismic Profilers and Echo Sounders (Anderson et al. 2007) emit sonic pulses to locate the soil-water interface, and hence the scour depth, using a similar approach to the radar methods. A variety of methods relies on the installation of rods into the soil near a foundation. Magnetic Sliding Collars (MSC) (Hunt, 2009) involves monitoring the movement of a gravity-controlled sensor which sits on the streambed surrounding a rod. The sensor falls with increasing scour depth relative to the rod and closes magnetic switches along the rod, which then indicates its depth. The Wallingford “Tell-Tail” Device (De Falco & Mele, 2002) consists of motion sensors tethered to a rod that detect bed movements as sediments are scoured to their level. Zarafshan et al. (2012) developed a system, which uses changes in the vibration frequency of a driven rod to detect scour, as measured using a Fibre-Bragg Grating (FBG) sensor.

Prendergast and Gavin (2014) note that most of the indirect methods are limited because they only gave information when scour has already occurred (and it may be too late to intervene) or they cannot be used during periods of flooding, when scour failures are most likely to occur.

### Indirect Methods

Indirect monitoring methods broadly refer to the use of the response of the structure to scour to detect the presence of scour. Most of these methods involve measuring the dynamic response of a bridge or bridge element using an accelerometer or otherwise, and observing how modal properties change when the foundation stiffness is compromised by scour. A variety of authors have investigated various aspects of the potential applicability of these approaches, in (Briaud et al. 2011, Chen, et al. 2014, Elsaid and Seracino, 2014, Foti and Sabia, 2010, Klinga and Alipour 2015 and Prendergast, et al. 2013).

Accelerometers allow the structural response to a change of boundary conditions to be directly measured. Whilst scour will increase the free length of a bridge pier founded in a water body, an effect which is simple to quantify, an additional soil-structure interaction effect occurs which is highly non-linear and therefore more difficult to quantify, See **Figure 17**. Any loss of material from beneath the footing will result in an increase in stress on the remaining soil. Since the soil-stiffness reduces as the strain-level increases, the global stiffness of the foundation will decrease significantly. The process illustrated for a shallow foundation below is equally applicable to pile foundations as load-redistribution will occur towards the pile tip. Measurement of the vibration response using an accelerometer can then be used to quantify the change of model characteristics (e.g. (frequency, mode shapes, derivatives of mode shapes, modal damping etc.).

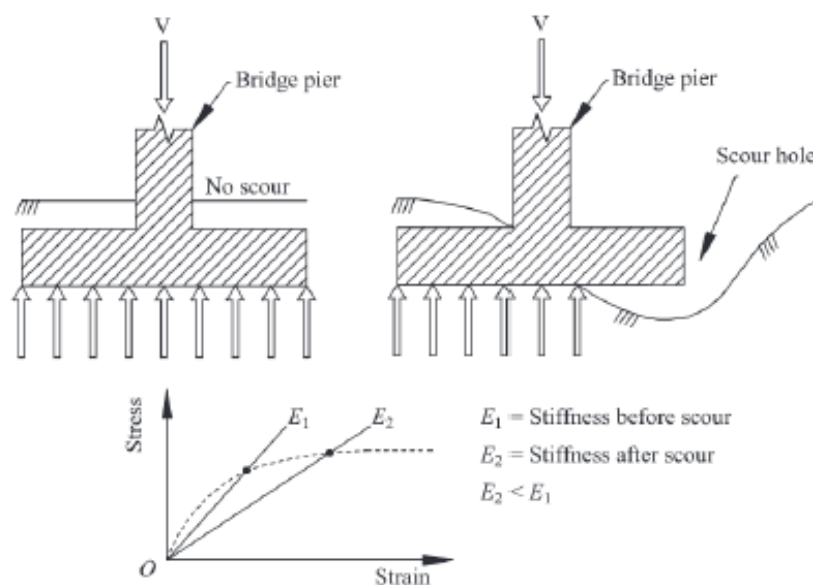


**Figure 17** Impact of scour on the stiffness of soil

Prendergast et al. (2013) report a field trial performed to track the change in natural frequency of a pile installed in dense sand during scouring. A 340mm diameter, open-ended steel pile was driven to a penetration depth of 7m below ground level. Four accelerometers were fitted along the initial exposed length and a data-logger recorded their output at a frequency of 1000Hz. A series of 0.5m deep scour holes were excavated until the scour hole depth was 6m, See **Figure 18a**. At each level, a lateral impulse force was applied to the top of the pile using a modal hammer and the transient acceleration response was recorded. In the experiment the



change of first natural frequency of the pile was recorded and compared to the result of a numerical model that modelled the pile as a beam element supported by a series of Winkler Springs, See **Figure 18b**. The primary input for the model, given the dynamic nature of the problem is the small-strain stiffness of the soil. A range of possible input values was considered from the API (1987) offshore design code, to direct measurement using MASW or indirect correlation to an in-situ Cone Penetration Test (CPT). The scour process was modelled by incremental removal of the springs, which assumes global scour has occurred.

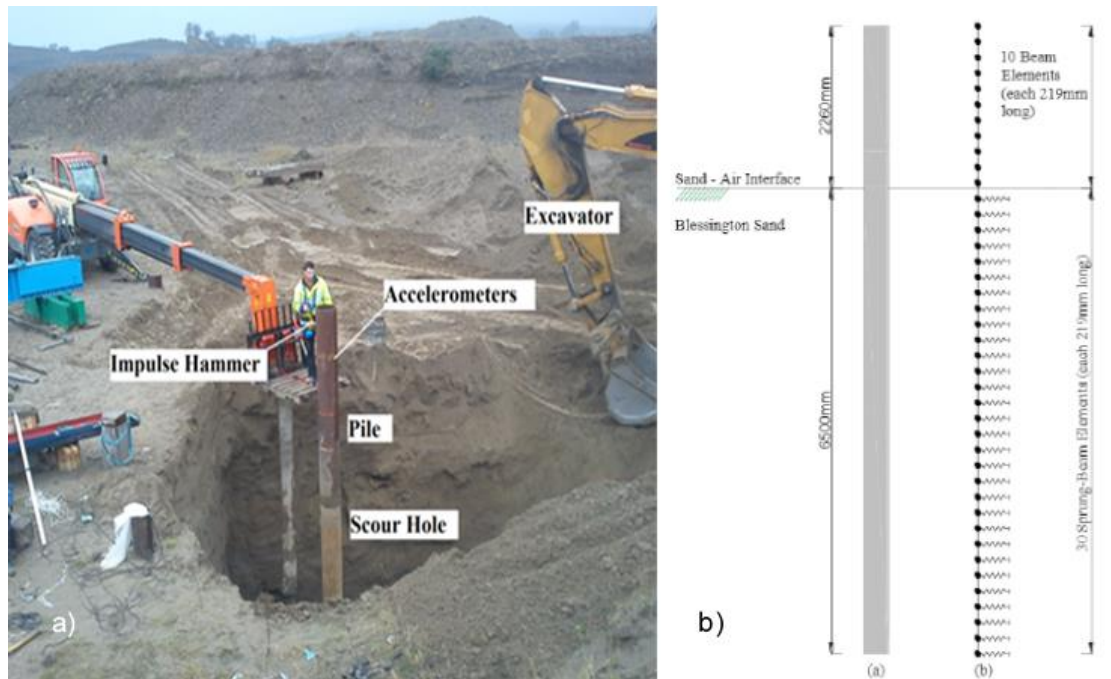


**Figure 18** a) Field test b) Numerical model

The measured and predicted frequencies throughout the scour process are shown in **Figure 19**. From the data it is clear, that:

1. The measured (experimental) natural frequency of the pile reduced from 33 Hz for a non-scoured pile to approximately 2 Hz when the scour depth reach 6m.
2. The numerical model that used the shear stiffness measured from the MASW test and inferred from the CPT profile provided excellent predictions of the non-scoured natural frequency and tracked the changes in natural frequency throughout the entire scour history. The close correlation between the MASW and CPT derived profiles at the site is unsurprising given that a site-specific correlation was established for these parameters, Gavin and Lehane. (2007) and Igoe and Gavin (2019).
3. The numerical mode that used the code-based API stiffness underestimated the initial natural frequency of the pile as it assumed a linear increase in soil stiffness with depth, which is conservative in an over-consolidated deposit.

Based on the field trial the method shows great promise in monitoring scour in real-time.

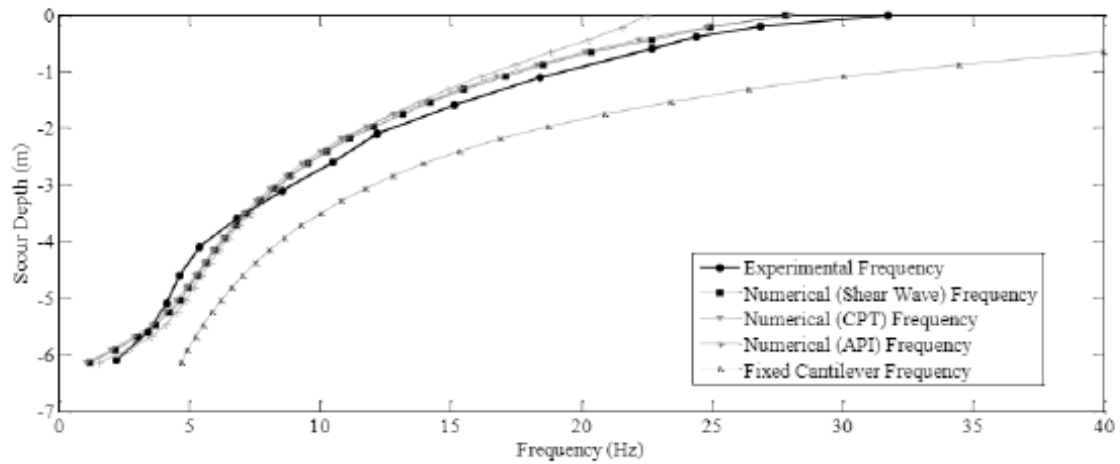


**Figure 19** Comparison of measured frequency with estimate from a numerical model

In order to assess potential of the method in real-world conditions Prendergast et al. (2016a, 2016b) developed numerical models to investigate the impact of scour at the central pier of a two-span integral bridge on the natural frequency response. The work considered the sensitivity of parameters such as vehicle speed and mass, road surface roughness and the impact of sensor noise on the vibration response. The work suggested that monitoring frequency changes showed potential to detect scour. Prendergast et al. (2017) further developed a novel Vehicle-Bridge-Soil Interaction (VBSI) model to generate realistic acceleration signals from the structure due to a two-axle truck travelling at typical highway speeds (80 km/hr.). The acceleration response at the top of the central pier of a pile supported structure with the soil stiffness varying from a loose to a dense state was tested. Results indicate that for all three soil stiffness profiles modelled the response signals generated were sufficient to allow the changes in natural frequency caused by scour (modelled using spring deletion) to be detected. Moreover, the shape of the scour depth versus frequency response plot was insensitive to soil state.

Shinoda et al (2008) and Liao et al. (2016) used the ratio between the current natural frequency of a bridge and the theoretical or initial natural frequency as an indicator for scour used to determine maintenance activities. A ratio less than 0.7 requires urgent maintenance, a ratio between 0.7 and 0.85 requires further investigation/monitoring, between 0.85 and 1 is classified as a minor problem. Kariyawasam et al. (2019) deployed a vibration-based monitoring system on the Baildon bridge in the UK, a 20m wide, 3-span concrete highway bridge in the UK, that had suffered scour damage as confirmed by diver inspections and sonar scanning, See **Figure 20**. The maximum depth of a scour hole was 1.8m at the right-hand side bridge pier.

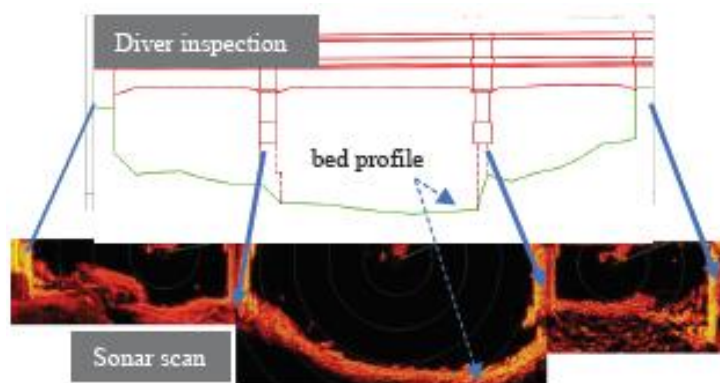


**Figure 20** Elevation of the maximum scour levels as shown in the dive inspection report and in sonar imagery (from Kariyawasam et al. 2019)

A numerical model of the bridge suggested that the natural frequencies were relatively high and high-sensitivity and low-noise accelerometers were deployed to capture scour sensitive longitudinal modes, see **Figure 21**. The response of the bridge as the scour holes were filled-in (scour in reverse) was recorded in the experiment.

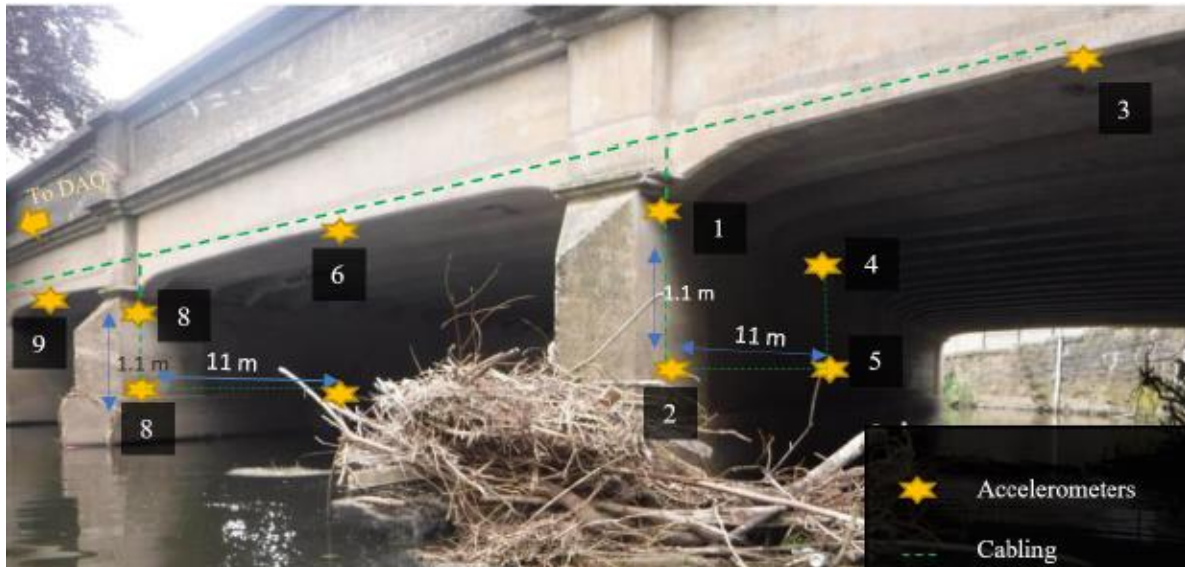


**Figure 21** Sensor positions on Baildon bridge (from Kariyawasam et al. 2019)

The numerical model suggested that the natural frequency of the bridge would vary between 0.14 and 0.54 Hz during filling of the scour holes. Analysis of the vibration data with a peak picking method and frequency domain decomposition gave a measurement error of 0.6-0.8 Hz. As a result, the resolution of natural frequency measurement was too low. However, there was a clear change in the mode shapes and power spectral density (PSD) of the accelerometer data for Mode 2 (Pier and deck Bending) during the repair phase between August and November, See **Figure 22**. In contrast the PSD of Mode 1 (1<sup>st</sup> sway mode) remains unchanged over the period, albeit with some noticeable outliers.

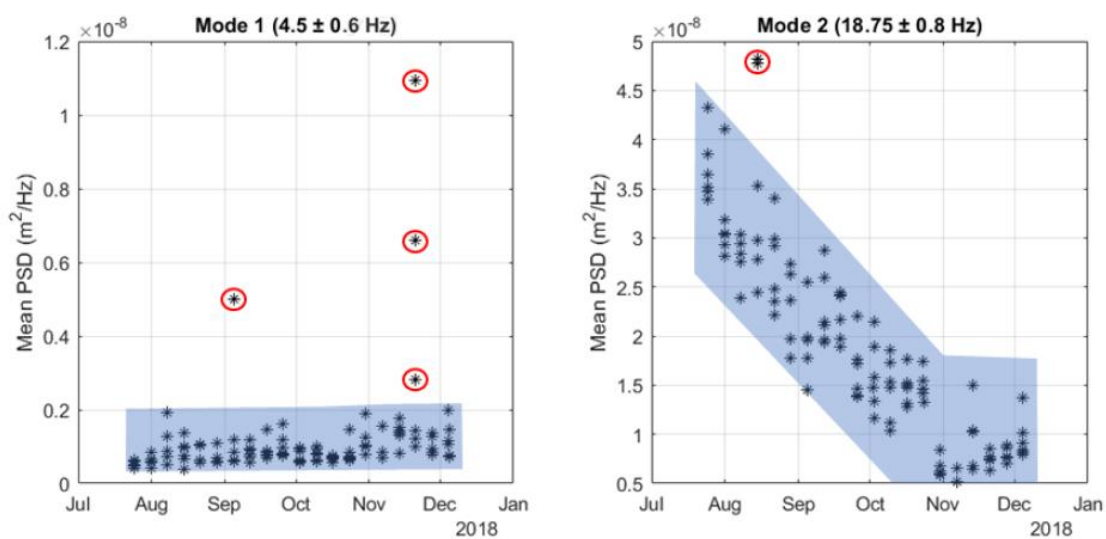


**Figure 22** Mean PSD of vibrations measured on the South Pier of Baildon bridge during scour-hole filling, (from Kariyawasam et al. 2019)

## 5 New technologies and examples of their application

### 5.1 Introduction

In the previous sections we identified some existing techniques for damage detection that are already widely used and focused on novel applications of these techniques in damage quantification. In this section we give a brief overview of some recently developed techniques including Unmanned Aerial Vehicles, UAV photogrammetry, laser scanning or using hybrids of all approaches that appear to have good promise in adding bridge and road management authorities.

### 5.2 Laser Scanning and UAV Photogrammetry

Recognizing the limitations of visual methods a number of workers have attempted to use digital image processing of data collected using optical techniques McRobbie et al. (2010) suggest that inspections based on 3D bridge information could completely simulate manual on-site observations. Optical sensors can be classified as either active or passive. Active sensors emit energy and record reflected signals in order to provide depth information. Passive sensors use ambient light to capture information that can be post-processed, See Fathi and Brilakis (2011). Active systems include using Terrestrial Laser Scanners (TLS), infrared scanning (IS) and imaging with Red-Green-Blue-Depth (RGB-D) whereas passive approaches use close range photogrammetry (CRP), See Poposecu et al. (2019). Adhikari et al. (2013) note that 3D point clouds can comprise millions of 3D points with millimeter level accuracy. These allow the development of primitive 3D models facilitating measurement and graphical representation of the scanned object. Early applications of the techniques were in the development of geometry models of historic arch bridges, see **Figure 23** (Truong-Hong and Laefer 2014). By combining TLS with GPR Lubowiecka et al. (2009) provided information on internal structure of a historic bridge (including fill, layering, inclusions etc.).

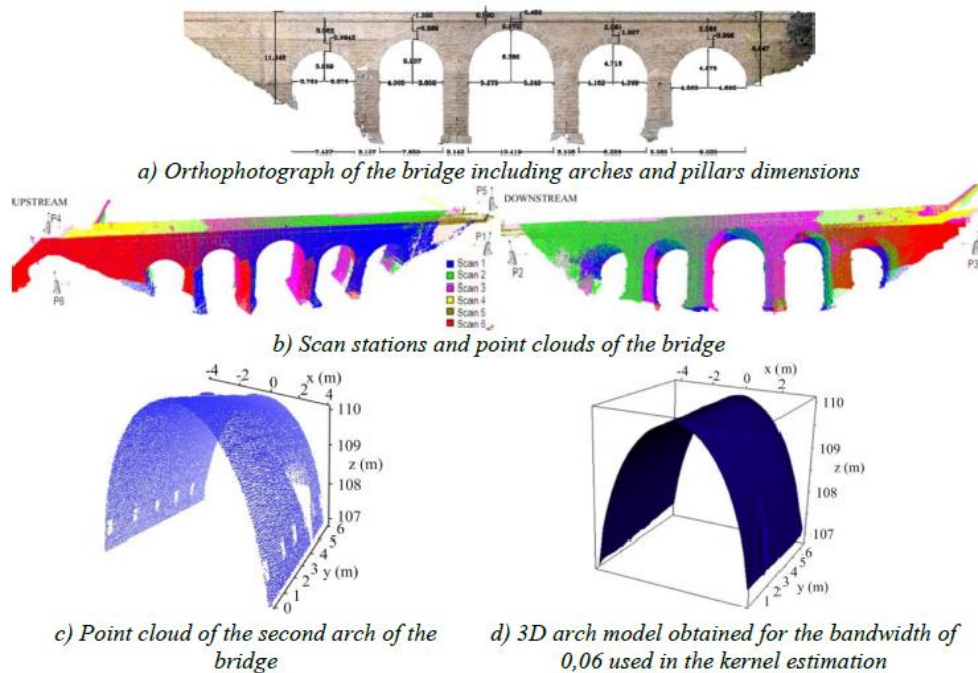


**Figure 23** Development of historic arch bridge models after Armesto et al. (2010)



The TLS technique has also been used to determine vertical deflections under load and clearance available under bridge soffits. The application in a number of damage detection studies showed that TLS can provide excellent data on spalling and cracking of concrete (Truong-Hong et al. 2016), with the capability to identify cracks as small as twice its sampling step. However, limitations include the high cost of equipment ( $\approx$ €25,000), limitations to full 3D scanning because of line of sight and the requirement to set-up on flat, stable terrain for setting-up the scanner.

As laser scanners create a record of spatial information of the bridges, the addition of photogrammetry allows additional information that is typically obtained from inspections. Jáuregui et al. (2005) demonstrate the creation of a 3D bridge model from still photographs using QuickTime Virtual Reality. Poposecu et al. (2019) compared three optical methods (TLS, CRP and IS) for creating 3D bridge models for a database of six railway bridges in Sweden. The authors created a 3D model of each bridge, first comparing the level of detail captured, See **Figure 24**. In general, the models created by TLS provided the highest level of detail with IS providing the lowest. The main dimensions, span, height etc. were captured by all methods. However, since the photogrammetry-based methods collected RGB data, more natural visualization was obtained.

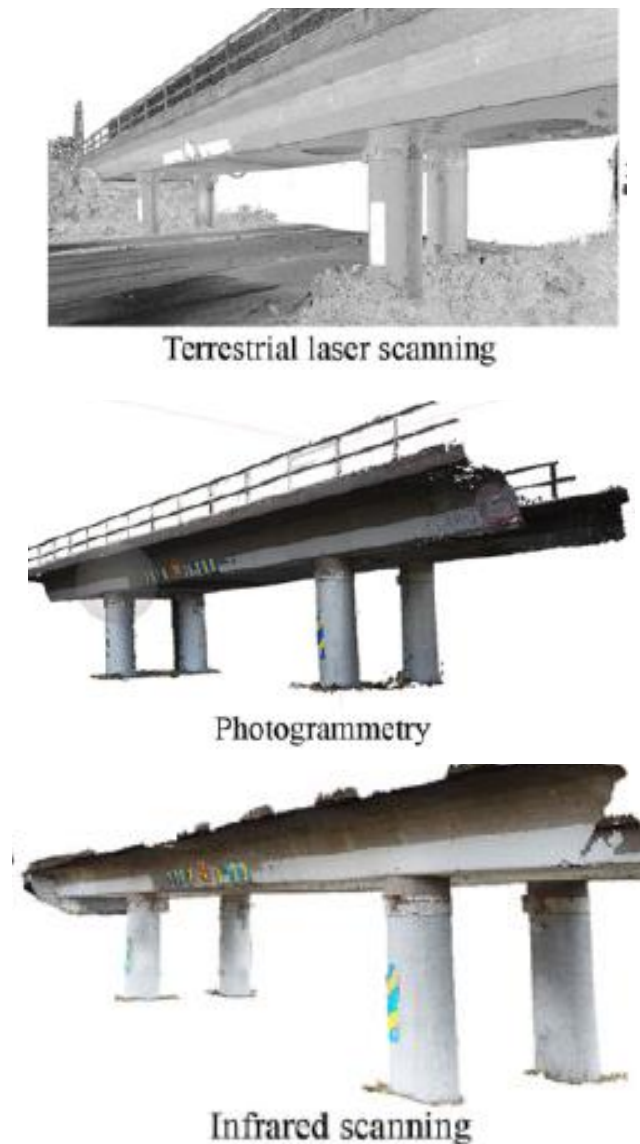


**Figure 24** 3D Models of Kallkallevagen bridge – showing different levels of detail obtained between TLS, CRP and IS (from Poposecu et al. (2019))

In order to check how sensitive the results of the photogrammetry-based methods are on the skills of the people performing the survey, the authors produced three models of the Pahtajokk bridge, the final bridge surveyed. Model 1 was based on photographs taken by and processed by post-graduate students whose experience consisted of scanning the five previous bridges in this study. The photos were taken with a Canon 5D camera and the data was processed using Agisoft PhotoScan Pro+ software. Model 2 was created using the photos taken for Model 1 and was processed using Bentley ContextCapture+ Software by experienced engineers. Model 3 was photographed by the experienced engineers using a Canon 5D Mark II camera and processed using the same software as Model 2. The results of the three models are shown in **Figure 25**. The results of all models are broadly similar suggesting that the model development is not very sensitive to the experience of the survey team.

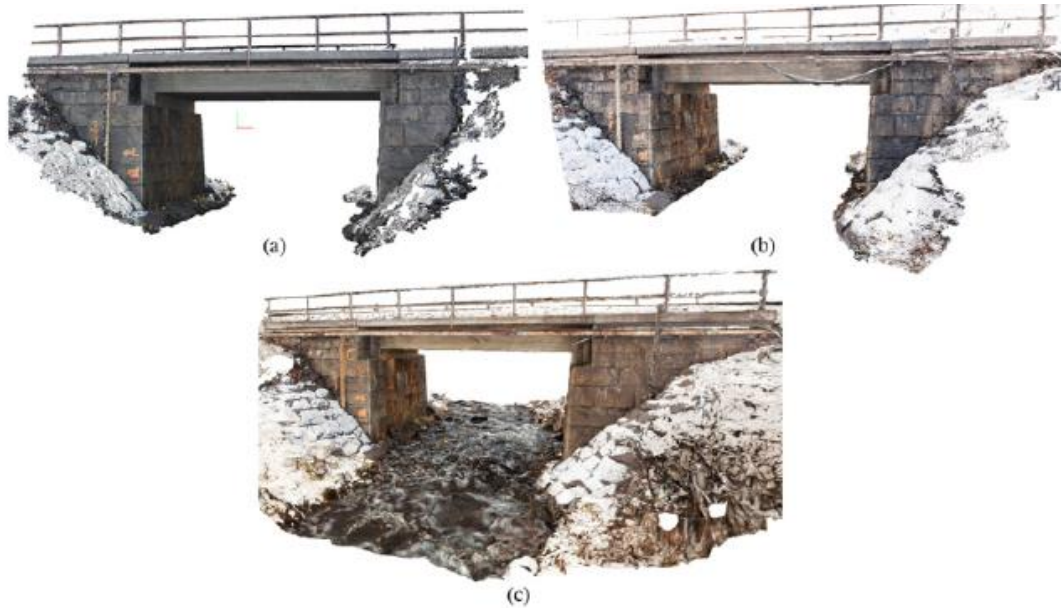


**Figure 25** CRP Models of Pahtajokk bridge developed using Model 1, 2 and 3  
(from Poposecu et al. (2019))

Solain et al (2020) present a case study to demonstrate the application of a semi-automated (automatic processing with manual validation) framework. The approach uses as input a point cloud collected using a mobile mapping system, and outputs an IFC file that represents the centre-line of the road and of each carriageway. To do this, the authors developed a method for detection and classification of solid and dashed road markings, a process for converting the main alignment and offset alignment from the point cloud processing method to an IFC Alignment model, which is part of the IFC 4.1s. In the anonymous case study area, a highway was surveyed with a LYNX Mobile Mapper by Optech and a LadyBug 5 panoramic camera (See Puente et al. 2013 for technical details of the scanner). The workflow developed to convert the point cloud data is shown in **Figure 26**.

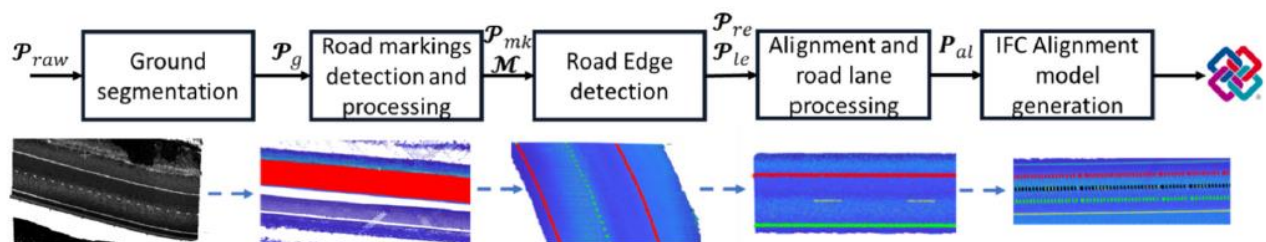


**Figure 26** Workflow to convert point cloud data to carriageway model (Solain et al. (2020))

The ability of photogrammetry to allow real-time damage detection was investigated by Jahanshahi et al. (2011) who deployed a fixed camera system for bridge inspection using a Canon PowerShot A610 that was capable of measuring crack widths of 0.57 mm for a camera 3m from the target. A drawback of these systems is line of sight, the need for the camera to be relatively close to the target and the cost of installation and maintenance, Lueker and Marr (2014).

Chen et al. (2019) present a case study where a low-cost drone is used to scan a bridge and allow a subsequent inspection using a 3D model of the bridge. Specifically, the paper deals with data acquisition, model reconstruction, and data quality determination. The methodology is applied in a scan on the Boyne Viaduct in Ireland, where the UAV scan performed using a DJI Phantom 4 with a 12-megapixel digital camera was compared to a TLS scan performed using a Leica Scan Station P20. The TLS survey only covered the side of the bridge as it was not possible to obtain access to the live rail line on the bridge deck. The 3D model was created from 153 images using Photoscan software. A series of data evaluation methods were proposed to quantify the point cloud performance in data completeness, density distribution, outlier noise level, surface deviation, and geometry accuracy. The authors concluded that the UAV offered significant advantages in data coverage, equipment cost and surveying time. However, challenges remain with regard to lower geometry accuracy than TLS and the long post-processing times required.

Isailović et al. (2020) present an approach for using point cloud data to detect spalling damage on bridges and further integrating damage information into a BIM model by semantic enrichment of an as-built IFC model. The steps required, (See **Figure 27**) include (i) Validation of the point-cloud data using either as-designed or preferably as-built model.

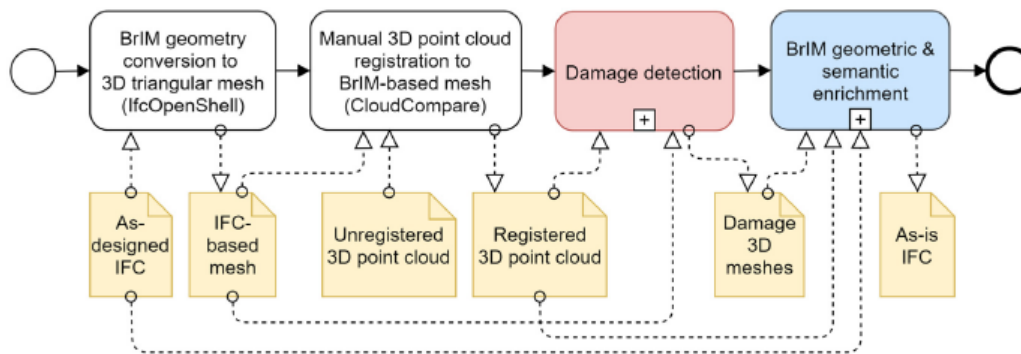
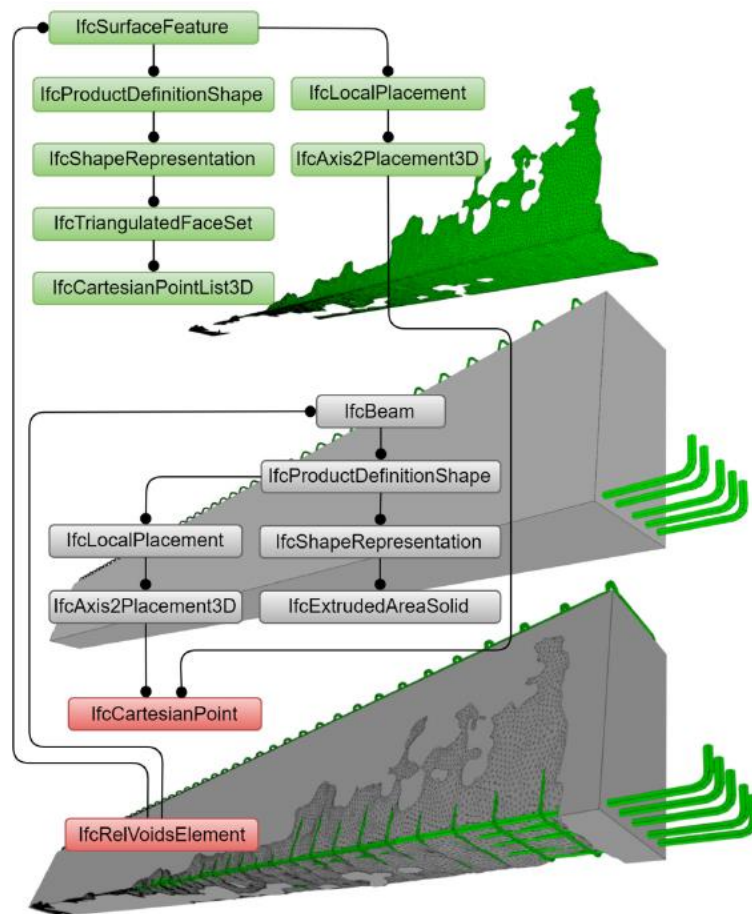


Fig. 1. Proposed BPMN process map of as-is BrIM generation.

**Figure 27** Methodology for detecting damage from point cloud data and incorporation as semantically rich data in BIM model of bridge (Isailović et al. 2020)



**Figure 28** IFC structure for geometric representation of damage (Isailović et al. 2020)

Guisado-Pintado et al. (2019) compared the efficacy of creating 3D maps for creating ground models of beach-dune zones using a drone and terrestrial laser scanner. They found both methods provided good topographic information with total survey times being lower for the UAV. Kim et al. (2015) presented a study on the use of a camera-based UAV system for concrete bridge surface crack detection. In their research, a morphological algorithm was designed for detecting and measuring crack widths, which resulted in a highly variable error (3–50%). However, in this fast-changing field, significant improvements occur frequently in terms of both hardware and software. As an example Oats et al. (2017) used a thermal camera for subsurface delamination and detection of damage in concrete. In their case study, they generated thermal and visible images for a 968-m<sup>2</sup> area, from which 14 m<sup>2</sup> of delamination was identified, which is an overall accuracy of about 95% compared with direct contact hammer sounding data.

### 5.3 InSAR

Space-borne Synthetic Aperture Radar Interferometry (InSAR) uses electromagnetic imaging of surface of the Earth collected from satellites to monitor relative deformations. The technology initially had resolution problems that meant it was most suitable for monitoring large-scale processes such as landslides and tectonic activity (Colesanti and Wasowski 2006, Colesanti et al. 2003). Recent developments in the interpretation have meant that resolutions are now appropriate for monitoring infrastructure such as bridges. In addition, the availability of historic data means that it is possible to look-back and investigate historic settlement behavior, with SAR capable satellite data being available from 1992 (Bianchini-Ciampoli 2020).



Mililli et al. (2019) present a methodology for interpretation of InSAR data and adoption of a Markov Chain Monte Carlo (MCMC) approach to determine pre-failure deformation of the Polcevera viaduct (known as the Morandi Bridge) in Italy. The multi-span bridge constructed opened in 1966 includes A-shaped frames (Pier No's 9 to 11 in **Figure 29**). The bridge was built between 1960 and 1966. A detailed inspection performed in 1993 identified a number of defects including damage to the oxidation of the metallic membrane protecting the strands Pier 11. Significant remedial works were performed on this Pier whilst replacement of the strands for the Pier 9 was planned to start in October 2018. On August 14<sup>th</sup> 2018 Pier 9 failed causing a 240m section of the bridge deck to collapse with 43 fatalities.

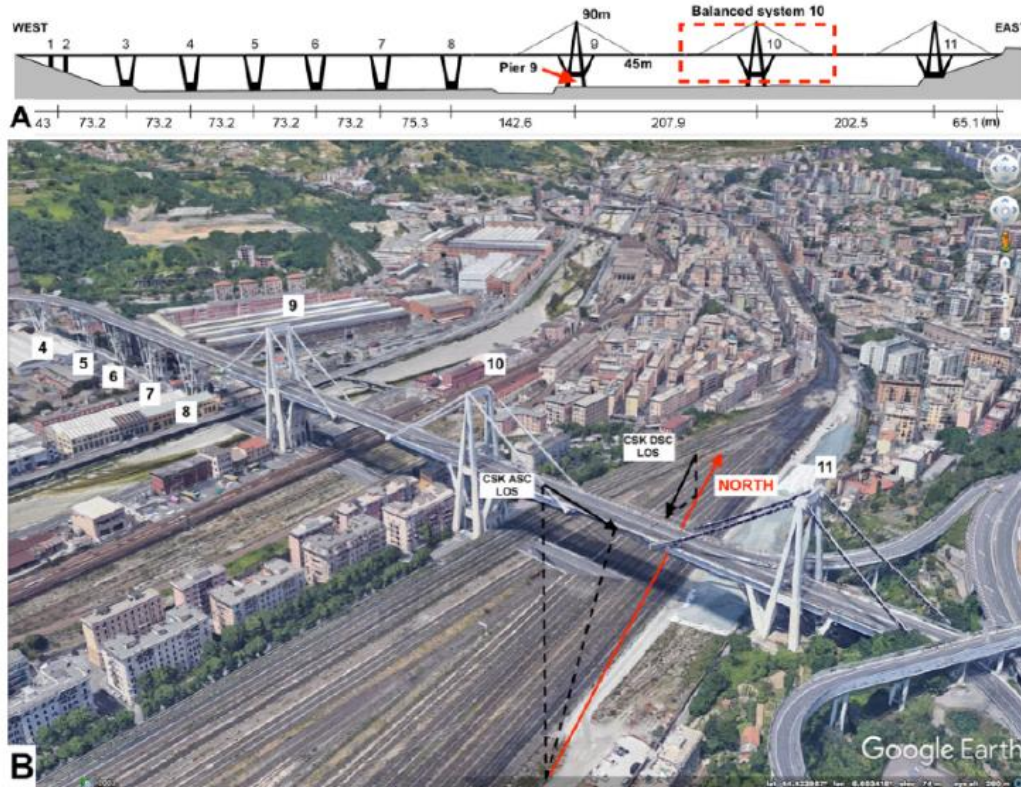


**Figure 29** The Morandi bridge pre-collapse showing the three A-Frame piers (after Mililli et al. 2019)

The line of sight data from 2009 until failure was utilized with a Markov Chain Monte Carlo (MCMC) approach to infer 3D displacement fields at Piers 9-11. The data for piers 9, 10 and 11 are shown in **Figure 30a**. At all locations displacements that increased linearly with time (at rates typically below 10mm/yr.). Pier 9 experienced a ten-fold increase in the rate of displacement, See **Figure 30b** in March 2017. The study thus indicated that whilst InSAR data cannot distinguish between stress accumulation and material degradation processes, it could be applied to detect changes in displacement behavior or structural distress of bridges.

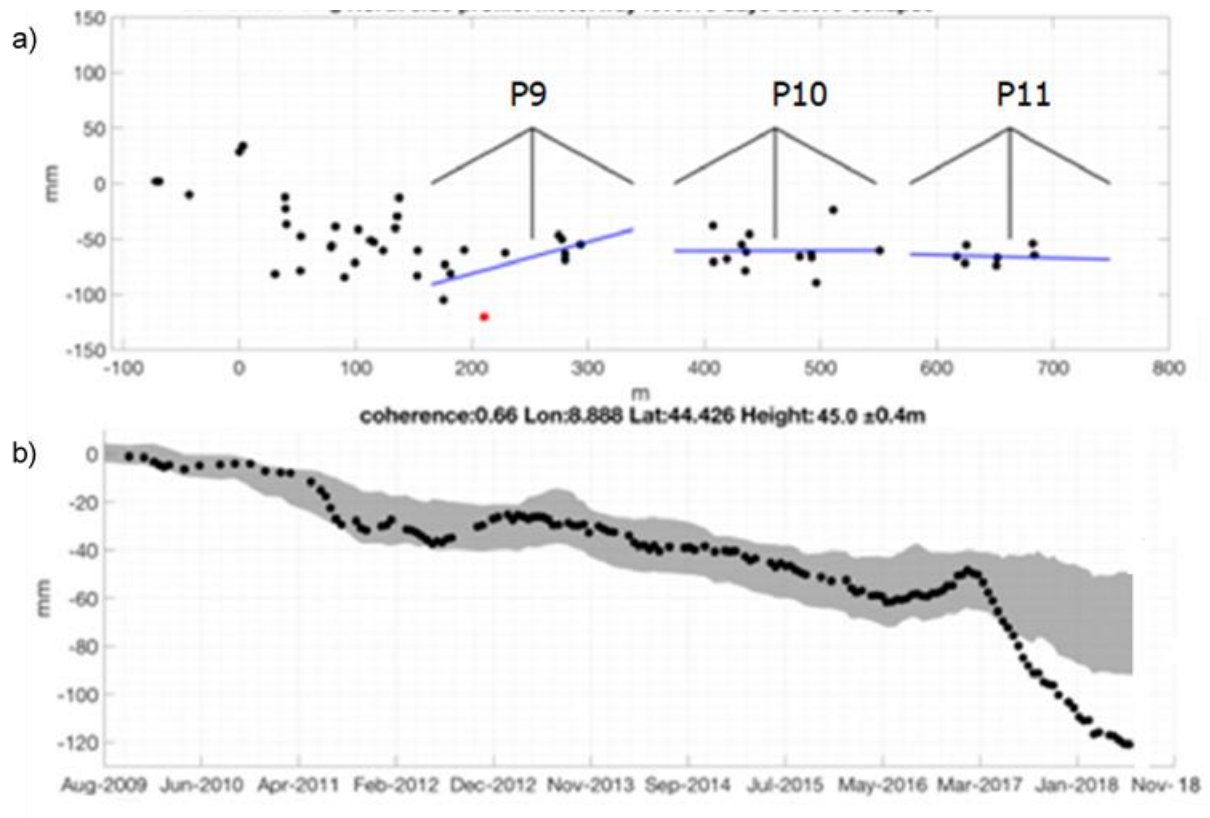


**Figure 30** Time-series deformations on Piers 9,10 and 11 based on CSK/Sentinel 1 A/B satellites from Mililli et al. (2019)

#### 5.4 UMVs for the detection of Scour

There are promising technologies that can measure the sea/river beds: bathymetric LiDAR and multi beam sounding deployed on Unmanned Marine Vehicles (UMVs). Murphy et al. (2011) describe the use of the Sea-RAI Unmanned Submersible Vehicle (USV) to undertake a post collapse inspection of the bridge substructure at the site of the Rollover Pass bridge in Texas which collapsed during Hurricane Ike in 2008. Three surveys were conducted, each lasting approximately 2 hours. The survey provided excellent images, see Figure 31 (in particular part c where bright sharp lines mark the interface between the pile foundation and the river bed) indicating no scour around the existing foundations.

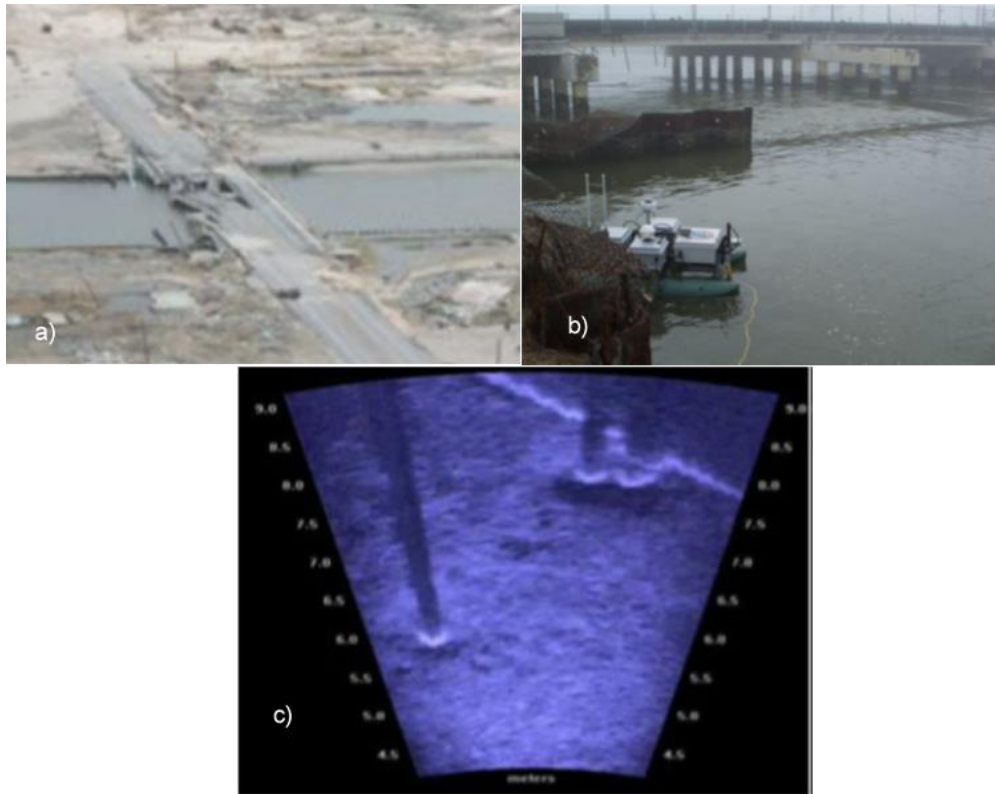


**Figure 31** a) Test site at Rollover Pass bridge in the US, b) The Sea-RAI UUV used in survey and c) Results showing no-scour at remaining bridge piers after Murphy et al. (2011)

Clubley et al. (2015) combined sonar and marine laser technology in a survey of a railway viaduct crossing the River Hamble in the UK. A desk-based risk assessment has classified the bridge as a medium scour risk. Therefore a diving inspection every four to six years was required. These investigations identified no scour at the bridge or notable changes in the river bed profile over time. In contrast the multi-beam sonar survey identified erosive scour at the bridge piers, see **Figure 32** where dark regions identify the presence of erosive scour features.

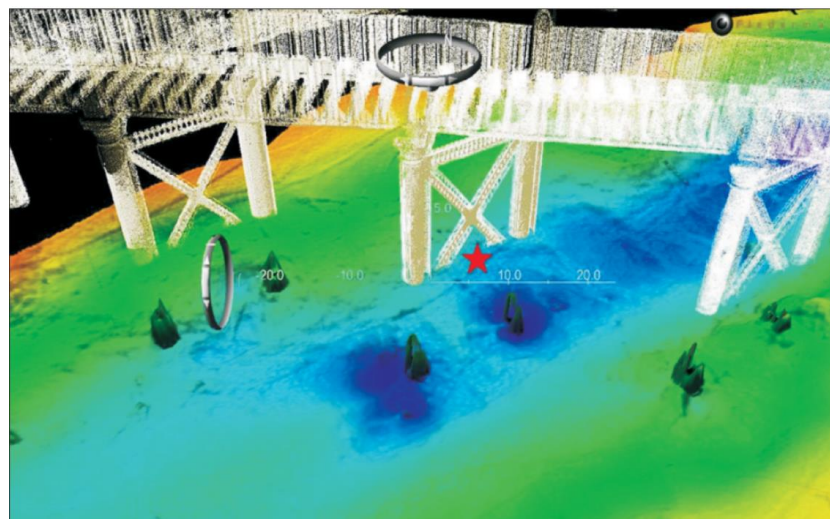


**Figure 32** Multi-beam sonar survey with marine laser structural overlay (Clubley et al. 2015)



## 5.5 Data fusion

In this section some examples of how data fusion can be used to enrich condition assessment are given. Endesley et al. (2012) describe a Decision support system for integrating remote sensing data to allow real-time bridge condition assessment. Gkoumas et al. (2019) See **Figure 33** identifies some of the novel techniques that could be used to feed such decision systems. Additional examples of data fusion that could be use in the decision making for road owners are described briefly below.

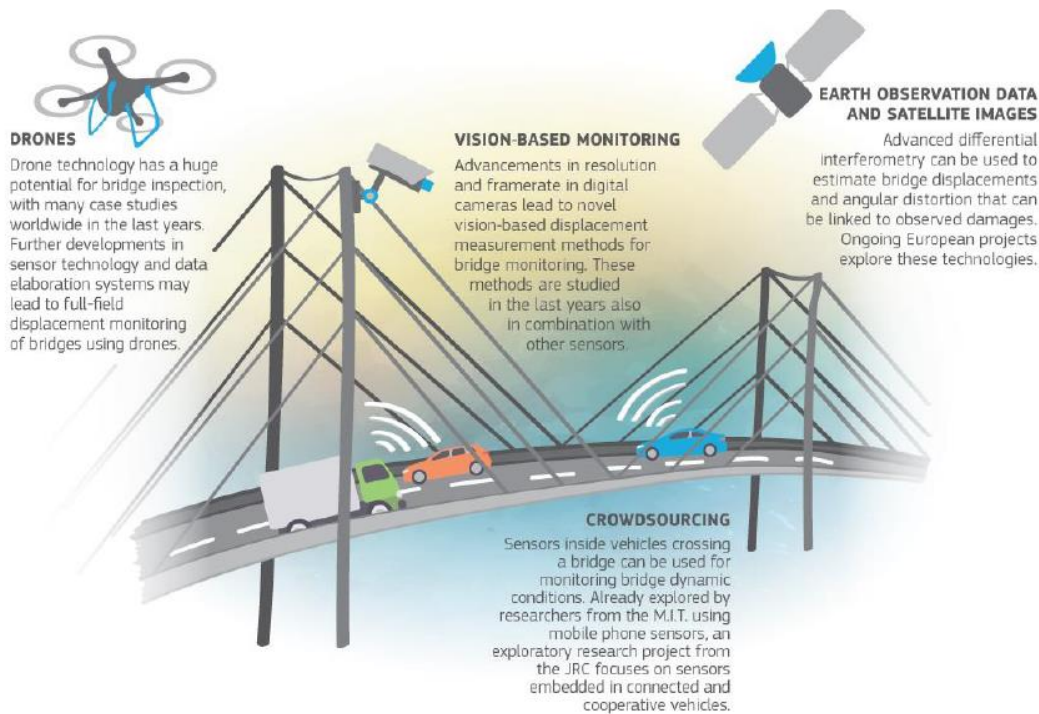


**Figure 33** Novel sources of data to provide input for bridge decision support systems (after Gkoumas et al. (2019))

### Ground settlement

Because laser scanning cannot give information on internal degradation processes, Biancini-Ciampoli et al. (2020) propose the data fusion concept of combining Synthetic Aperture Radar (SAR) data with GPR to infer information about the material forming the structure. They performed a field investigation on a 9.8km section of the railway line in Foggia, Southern Italy. GPR acquisition was performed using a train mounted, multi-frequency antennae (1000 MHz and 2000 MHz). The InSAR data were collected by the Sentinel 1A mission between April 2017 and January 2018. The interpreted data revealed one location (red point in Figure 34a) where the displacement rate was in the range 20-24mm/yr. The GPR survey identified a number of high attenuation areas, associated with clayey, compressible materials in this area.

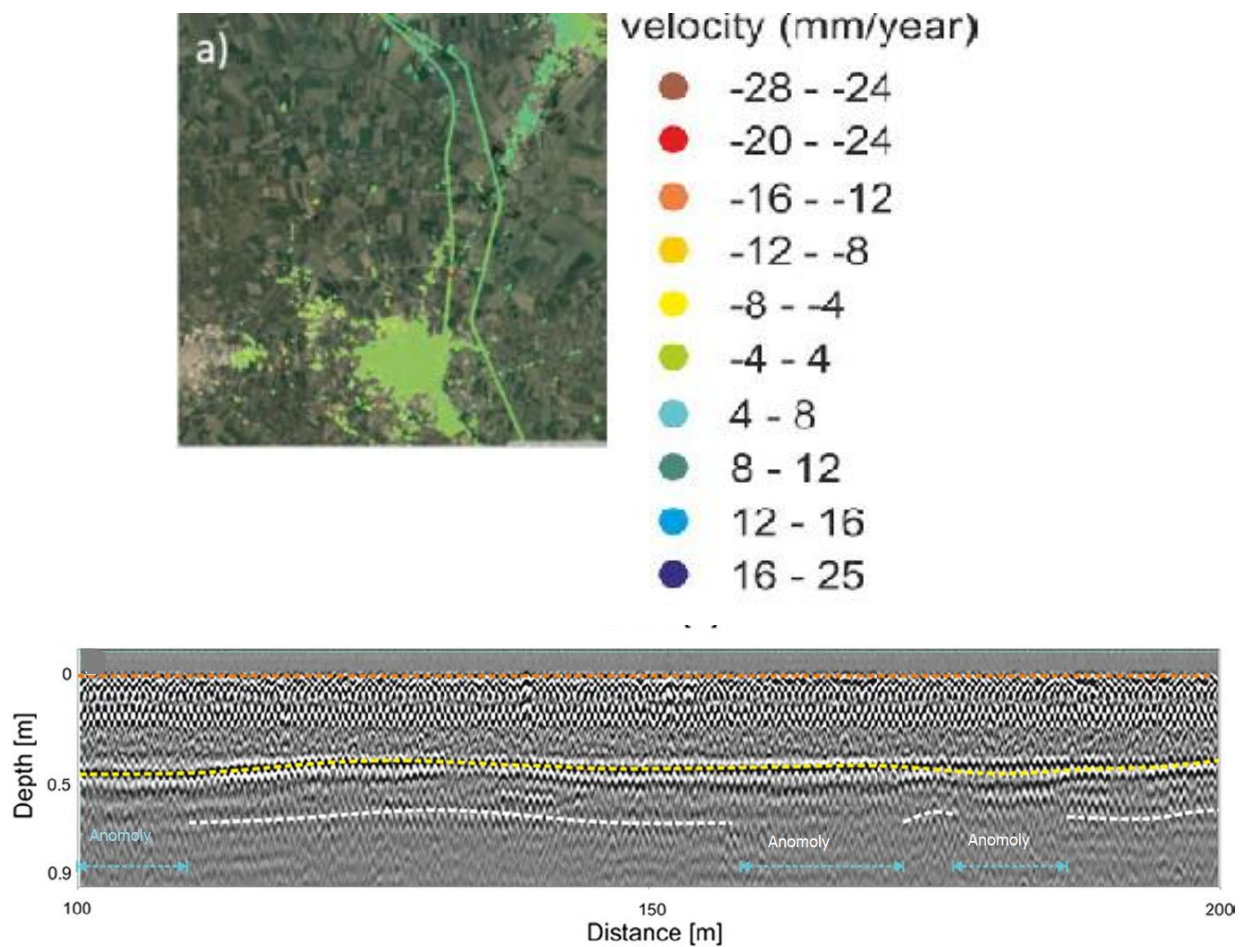


**Figure 34** Data fusion of InSAR and GPR to locate and investigate subsidence on an Italian Rail line (Ciampoli et al. 2020)

### ***Condition assessment of embankments***

Kovacevic et al. (2019) describes a methodology to first determine the current condition of embankments using a combination of ground penetrating radar (GPR) surveys, visual inspection, and historical data about maintenance activities. These attributes were then used for the development of a multi-attribute utility theory model used as a support for decision making process for maintenance planning. The methodology was demonstrated for the condition categorization of 181 km of embankments on the Croatian transport network. The GPR data was obtained using a combination of high-frequency antennae (at least 1 GHz) to investigate shallow features such as ballast pockets and ballast quality (fouling) and lower frequency antennae, for example up to 400 MHz (depending on the embankment height), to map deep irregularities within the sub-base and embankment material.

## 6 Conclusions

It is necessary to assess the physical and functional conditions of critical assets such as road pavements and highway bridges at regular intervals to ensure they still meet their service requirements. Whilst automated systems have been developed for pavement evaluation in the case of bridges this condition assessment continues to be mainly performed through visual inspection. A number of studies have highlighted the limitations of this approach. In the modern era where climate stressors affect our infrastructure, degradation of condition can be rapid and we need to harness new technologies to maintain safety and maximize mobility.

The report identifies a number of technologies that can produce direct or in-most cases indirect measures of damage to roads and bridges. It is apparent that certain techniques are reaching high technology readiness levels for measuring specific quantities. Given each method's unique abilities there is growing interest in combining technologies and fusing data to allow owners to get a complete picture of their assets. In road assessment products as the Fugro Automatic Road Analyser<sup>1</sup> are already commercially deployed. This offers a range of measurements from a single survey including; Digital imaging, GPR, rutting, texture and distress data. In the bridge management sector, there is key research ongoing in the fusion of digital images/scans for creation of accurate 3D models and identifying damage using advanced machine learning algorithms.

As a first-step to allowing road owners utilize the technologies described in the report, a structured approach to collecting and storing the data in a transparent manner that allows engineers to manipulate data for modelling is essential. A Building Information Model (BIM) provides a single source of information, storing data including geometry, state etc. of an asset. With the inclusion of data from a range of sources included in this report a BIM model can evolve as an asset ages (Boorman et al., 2018).

The information collected in this deliverable will set the foundation for further work of the project in the sense of providing input on the following parameters; what should be measured, where should the measurement be performed, what format and frequency of data should be collected. Ultimately the BIM models will be designed to accommodate this information and allow informed condition assessment and decision making.

---

<sup>1</sup> <https://www.fugro.com/our-services/asset-integrity/roadware/aran-automatic-road-analyze>

## 7 Bibliography

- Adhikari, R. S., O. Moselhi, and A. Bagchi, 2013, Image-based retrieval of concrete crack properties for bridge inspection.: *Automation in Construction*, v. 39, p. 180-194.
- Aleotti, P., Chowdhury, R., 1999. Landslide hazard assessment: summary review and new perspectives. *Bull. Eng. Geol. Environ.* 58 (1), 21–44.
- Anderson, N. L., A. M. Ismael, and T. Thitimakorn, 2007, Ground-Penetrating Radar: A Tool for Monitoring Bridge Scour.: *Environmental and Engineering Geoscience*, v. 13, p. 1-10.
- Armesto, J., Roca-Pardiñas, J. Lorenzo, H. and Arias, P. (2010) Modelling masonry arches shape using terrestrial laser scanning data and nonparametric methods, *Engineering Structures* 32 607615.
- Arneson, L. A., Zevenbergen, L. W., Lagasse, P. F., and Clopper, P. E. (2012). "Evaluating scour at bridges (HEC-18)." Technical Rep. No. FHWA (Federal Highway Administration) HIF-12-003, Washington, DC.
- Azari, H., and Lin, S. (2019). Evaluation of the Impact Echo Method for Concrete Bridge Decks with Asphalt Overlays, *Transportation Research Record*, February 12, 2019 Research <https://doi.org/10.1177/0361198119828676>
- Bahrani, N., Blanc, J. Hornrych, P. and Menant, F. (2020) Alternate Method of Pavement Assessment Using Geophones and Accelerometers for Measuring the Pavement Response, *Infrastructures*, Vol.5, No. 25. doi:10.3390/infrastructures5030025.
- Bianchini Ciampoli, L.; Tosti, F.; Economou, N.; Benedetto, F. (2019) Signal Processing of GPR Data for Road Surveys.*Geosciences*, Vol,9, No.96
- Bianchini Ciampoli, L., Gagliardi, V. Clementini, C. Latini, D. Del Frate, F. and Benedetto, A. Transport Infrastructure Monitoring by InSAR and GPR Data Fusion, *Surveys in Geophysics*, 1-24, 2019
- Borrmann, A.; König, M.; Koch, C.; Beetz, J. (2018) *Building Information Modeling: Technology Foundations and Industry Practice*; Springer: Berlin, German.
- Briaud, J. L., Hurlbaas, S., Chang, K. A., Yao, C., Sharma, H., Yu, O. Y. and Price, G. R. (2011). Realtime monitoring of bridge scour using remote monitoring technology. Texas Transportation Institute, Texas A&M University System.
- Briaud, J. L., Ting, F. C., Chen, H. C., Gudavalli, R., Perugu, S., & Wei, G. (1999). SRICOS: Prediction of scour rate in cohesive soils at bridge piers. *Journal of Geotechnical and Geoenvironmental Engineering*, 125(4), 237-246. [https://doi.org/10.1061/\(ASCE\)1090-0241\(1999\)125:4\(237\)](https://doi.org/10.1061/(ASCE)1090-0241(1999)125:4(237))
- Caris J.P.T. and Van Asch T.W.J. 1991. Geophysical, geotechnical and hydrological investigations of a small landslide in the French Alps. *Engineering Geology* 21, 249–276.
- CEDR (2015) Report No. WP2-M1 Identifying the key requirements for structural condition measurements, [www.cedr](http://www.cedr).
- Chen, C. C., Wu, W. H. Shih, F. and Wang, S. W. (2014). Scour evaluation for foundation of a cable-stayed bridge based on ambient vibration measurements of superstructure. *NDT & E International*, 66, 16-27. <https://doi.org/10.1016/j.ndteint.2014.04.005>

- Chen; S., Laefer,D.F, Mangina;E. Zolanvari;I and and Byrne, J. (2019) UAV Bridge Inspection through Evaluated 3D Reconstructions, ASCE Jrnl. of Bridge Engineering, April, Vol. 24, No.4
- Cheng, C.-C., T.-M. Cheng, and C.-H. Chiang, 2008, Defect detection of concrete structures using both infrared thermography and elastic waves: Automation in Construction, v. 18, p. 87-92.
- Clubley, S.K.; Manes, C.; Richards, D.J. (2015) High resolution sonars set to revolutionise bridge scour inspections. Proc. Inst. Civ. Eng. Civil Engineering,168, 35–42
- Codeglia, D., Dixon, N. Fownes, G.J. and Marcato, G. (2017) Analysis of acoustic emission patterns for monitoring of rock slope deformation mechanisms, Engineering Geology, 219, pp 21-31
- Colesanti C, Wasowski J (2006) Investigating landslides with space-borne Synthetic Aperture Radar (SAR) interferometry. Eng Geol 88(3–4):173–199. <https://doi.org/10.1016/j.enggeo.2006.09.013>
- De Falco, F., & Mele, R. (2002). The monitoring of bridges for scour by sonar and sediment. NDT & E International, 35(2), 117-123. [https://doi.org/10.1016/S0963-8695\(01\)00031-7](https://doi.org/10.1016/S0963-8695(01)00031-7)
- DMRB (2017) Design Manual for Roads and Bridges, BD 63/17Volume 3 Section 1, Part 4 – Inspection of Highway structures
- Donohue, S. Gavin, K. and Tooliyan, A. (2011). Use of geophysical techniques to examine slope failures,. Journal of Near Surface Geophysics. Vol 9, No.1, February, pp 33-44, DOI: 10.3997/1873-0604.2010040
- Donohue, S., Gunn, D.A., Bergamo, P., Hughes, E., Dashwood, B., Uhlemann, S., Chambers, J. E.andWard, D. [2014] Assessing climate effects on railway earthworks using MASW. Near Surface Geoscience 2014.
- Dong, Y., and F. Ansari, 2011, Non-destructive testing and evaluation (NDT/NDE) of civil structure rehabilitated using fibre reinforced polymer (FRP) composites.: Woodhead Publishing Series in Civil and Structural Engineering, v. Service Life Estimation and Extension of Civil Engineering Structures, p. 193-222.
- Dong, S. Ye, Y. Gao, G. Fang, X. Zhang, Z. Xue, T. Zhang, (2016) Rapid detection methods for asphalt pavement thicknesses and defects by a vehicle-mounted ground penetrating radar (GPR) system, Sensors 16 (2016) 1–18, <http://dx.doi.org/10.3390/s16122067>.
- Elsaid, A., & Seracino, R. (2014). Rapid assessment of foundation scour using the dynamic features of bridge superstructure. Construction and Building Materials, 50, 42-49. <https://doi.org/10.1016/j.conbuildmat.2013.08.079>
- Endsley, K. A., Brooks, C. Harris, D. Ahlborn, T. & Vaghefi, K. (2012). Decision support system for integrating remote sensing in bridge condition assessment and preservation. SPIE Smart Structures and Materials Nondestructive Evaluation and Health Monitoring, San Diego, California. , 8345
- Fathi, H., and Brilakis, I. (2011) Automated sparse 3D point cloud generation of infrastructure using its distinctive features, Advanced Engineering Informatics Vol. 25, No.4, pp 760-770.
- Fedele, R.; Praticò; F.G; Carotenuto, R.; Della Corte, F.G. Instrumented infrastructures for damage detection and management. In Proceedings of the 5th IEEE International Conference on Models and Technologies for Intelligent Transportation Systems, Naples, Italy, 26–28 June 2017, pp. 526–531, doi:10.1109/MTITS.2017.8005729.



- Fisher, M., Chowdhury, M. N., Khan, A. A., & Atamturktur, S. (2013). An evaluation of scour measurement devices. *Flow Measurement and Instrumentation*, 33, 55-67. <https://doi.org/10.1016/j.flowmeasinst.2013.05.001>
- Forde, M. C., McCann, D. M., Clark, M. R., Broughton, K. J., Fenning, P. J., & Brown, A. (1999). Radar measurement of bridge scour. *Ndt & E International*, 32(8), 481-492. [https://doi.org/10.1016/S0963-8695\(99\)00026-2](https://doi.org/10.1016/S0963-8695(99)00026-2)
- Foti, S., and Sabia, D. (2010). Influence of foundation scour on the dynamic response of an existing bridge. *Journal of bridge engineering*, 16(2), 295-304.
- Friedel S., Thielen A. and Springman S.M. 2006. Investigation of a slope endangered by rainfall-induced landslides using 3D resistivity tomography and geotechnical testing. *Journal of Applied Geophysics*60, 100–114
- Gastineau,A., Johnson,T., Schultz,A., 2009. Bridge health monitoring and inspections systems –a survey of methods.Department of Civil Engineering, University of Minnesota.
- Gavin, K., and B. Lehanç, 2007, Base load-displacement response of piles in sand: *Canadian Geotechnical Journal*, v. 44, p. 1053-1063.
- Gavin, K. and Xue, J. (2009) Use of a genetic algorithm to perform reliability analysis of unsaturated soil slopes. Gavin, K. and Xue, J. *Geotechnique*, Vol. 59, No. 6 , pp 545-549. DOI 10.1680/geot.8.T.004
- Gavin, K. and Xue, J. (2010) Design charts for the stability analysis of unsaturated soil slopes, *Journal of Geotechnical and Geological Engineering*, Vol 28 pp 79-90. DOI 10.1007/s10706-009-9282-z
- Gavin,K.,Prendergast, L.Stipanovič, I and S.Škarič (2018) Recent developments and remaining challenges in determining unique bridge scour performance indicators, *The Baltic Journal of Road and Bridge Engineering*, Vol. 13 pp.291–300 .
- Gkoumas, K., Marques Dos Santos, F.L., van Balen, M., Tsakalidis, A., Ortega Hortelano, A., Grosso, M., Haq, G., Pekár, F., (2019) Research and innovation in bridge maintenance, inspection and monitoring - A European perspective based on the Transport Research and Innovation Monitoring and Information System (TRIMIS), EUR 29650 EN, Publications Office of the European Union, Luxembourg, 2019, ISBN 978-92-79-99678-8, doi:10.2760/16174, JRC115319.
- Göktürkler G., Balkaya C. and Erhan Z. 2008. Geophysical investigation of a landslide: The Altındağ landslide site, İzmir (western Turkey). *Journal of Applied Geophysics*65, 84–96
- Godio A. and Bottino G. 2001. Electrical and electromagnetic investigation for landslide characterisation. *Physics and Chemistry of the Earth, Part C, Solar, Terrestrial & Planetary Science*26, 705–710.
- Gucunski. N., Consolazio, G.R. and Maher, A. "Concrete Bridge Deck Delamination Detection by Integrated Ultrasonic Methods." *International Journal of Materials and Product Technology*. 2006. Vol. 26. pp. 19-34.
- Guisado- Pintado, E., D. W.T. Jackson, and D. Rogers, 2018, 3D mapping efficacy of a drone and terrestrial laser scanner over a temperate beach-dune zone: *Geomorphology*
- Hajdin, R.Kušar, M; Mašović, S; Linneberg, P; Amado, J; Tanasić, N.; Ademović, N; Costa, C; Kušter Marić, M; Almeida, J; Galvão, N et al. (2018) COST TU1406 - Technical report of the

- Working group 3: Establishment of a Quality Control Plan, Guimaraes, Portugal: COST TU1406, 2018 (prirucnik) doi:10.13140/RG.2.2.28730.03526
- Hiasa, S. (2016). Investigation of infrared thermography for subsurface damage Investigation of infrared thermography for subsurface damage detection of concrete structures detection of concrete structures, PhD Thesis University of Central Florida <https://stars.library.ucf.edu/cgi/viewcontent.cgi?article=6063&context=etd>)
- Hugenschmidt, J., 2002, Concrete Bridge inspection with a mobile GPR system.: Construction and Building Materials, v. 16, p. 147-154.
- Hugenschmidt J, and Mastrangelo R. (2009) GPR inspection of concrete bridges. Journal of Cement Concrete Composites 2006; 28: doi.org/10.1016/j.cemconcomp.2006.02.016
- Hunt, B. E. (2009). NCHRP synthesis 396: monitoring scour critical bridges—a synthesis of highway practice. Transportation Research Board, Washington, DC.
- Igoe, D., and K. Gavin, 2019, Characterization of the blessington sand geotechnical test site: AIMS Geosciences, v. 5, p. 145-162.
- Isailović, D., V. Stojanovic, M. Trapp, R. Richter, R. Hajdin, and J. Döllner, 2020, Bridge Damage: Detection, IFC- based semantic enrichment and visualization.: Automation in Construction, v. 112.
- Israil M. and Pachauri A.K. 2003. Geophysical characterization of a landslide site in the Himalayan foothill region. Journal of Asian Earth Sciences22, 253–263
- Kariyawasam, K.K.; Fidler, P.R.; Talbot, J.P.; Middleton, C.R. Field Deployment of an Ambient Vibration-Based Scour Monitoring System at Baildon Bridge, UK. In Proceedings of the International Conference on Smart Infrastructure and Construction (ICSIC) Driving data-informed decision-making 2019, Cambridge, UK, 8–10 July 2019; pp. 711–719.
- Kim, H., S. H. Sim, and S. Cho. 2015. “Unmanned aerial vehicle (UAV) powered concrete crack detection based on digital image processing.” In Proc., 6th Int. Conf. on Advances in Experimental Structural Engineering, 11th Int. Workshop on Advanced Smart Materials and Smart Structures Technology, 1–2. Urbana, IL: Univ. of Illinois Urbana Champaign.
- Klose, M., Damm, B., Terhorst, B., 2015. Landslide cost modeling for transportation infrastructures: a methodological approach. Landslides 12 (2), 321–334.
- Kušar, M., Galvão, N. and Sein, S. (2019) Regular bridge inspection data improvement using non-destructive testing, In Life-Cycle Analysis and Assessment in Civil Engineering: Towards an Integrated Vision – Caspeele, Taerwe & Frangopol (Eds) 2019 Taylor & Francis Group, London, ISBN 978-1-138-62633-1
- Jahanshahi, M. R., S. F. Masri, and G. S. Sukhatme. (2011). Multi-image stitching and scene reconstruction for evaluating defect evolution in structures. Structural Health Monitoring Vol. 10 No.6: pp 643–657.
- Jáuregui, D. V., Tian, Y., & Jiang, R. (2006). Photogrammetry Applications in Routine Bridge Inspection and Historic Bridge Documentation. Las Cruces: New Mexico State University.
- Klinga, J. V., & Alipour, A. (2015). Assessment of structural integrity of bridges under extreme scour conditions. Engineering Structures, 82, 55-71. <https://doi.org/10.1016/j.engstruct.2014.07.021>
- Kongrattanasert, W., Nomura, H., Kamakura, T., & Ueda, K. (2010). Detection of road surface states from tire noise using neural network analysis. In IEEE Transactions on Industry Applications (Vol. 20, pp. 920– 925). doi:10.1541/ieejias.130.920

- Kovacevic, M.S., Basic, M, Kaynia, A, Noren-Cosgriff, K., Kassa, E. and Gavin, K.G. (2017) Guideline on Methods to Find Hot-Spots on Rail Networks, Deliverable 1.2 of EU H2020 Destination Rail project, [www.destinationrail.eu](http://www.destinationrail.eu)
- Lapenna V., Lorenzo P., Perrone A., Piscitelli S., Sdao F. and Rizzo E. 2003. High-resolution geoelectrical tomographies in the study of the Giarossa landslide (southern Italy). *Bulletin of Engineering Geology and the Environment* 62, 259–268.
- La Torre et al. (2007) COST 354 Performance Indicators for Road Pavements, Report on WP 2 Selection and assessment of individual performance indicators, COST354/WP2 Report No. 30052008
- Lekshmiopathy, J., N. M. Samuel, and S. Velayudhan, 2020a, Vibration vs vision: best approach for automated pavement distress detection. *International Journal of Pavement Research and Technology*, Vol. 13, pp 402-410.
- Li C, Ashlock J, Lin S, et al. In Situ Modulus Reduction Characteristics of Stabilized Pavement Foundations by Multichannel Analysis of Surface Waves and Falling Weight Deflectometer Tests. *Construction and Building Materials* 2018; 188: 809–819. <https://doi.org/10.1016/j.conbuildmat.2018.08.163>
- Liao, K., (2016) Preliminary bridge health evaluation using the pier vibration frequency, *Journal of Construction and Building Materials*, Elsevier, pp. 552-663.
- Lubowiecka, I., Armesto, J. Arias, P. and Lorenzo, H. (2009) Historic bridge modelling using laser scanning, ground penetrating radar and finite element methods in the context of structural dynamics, *Engineering Structures* 31 (11) 2667-2676.
- Lueker, M., and J. Marr. 2014. Scour monitoring technology implementation. MN/RC 2014-37. St. Paul, MN: Minnesota DOT.
- Marchetti, M.; Ludwig, S.; Dumoulin, J.; Ibos, L.; Mazioud, A. (2008) Active Infrared Thermography for Non-destructive Control for Detection of Defects in Asphalt Pavements. *Proceedings of QIRT 2008 (Quantitative Infrared Thermography)*, Krakow, Poland, July 2–5.
- Martinović, K., Gavin, K., and Reale, C., 2016. Development of a landslide susceptibility assessment for a rail network. *Eng. Geol.* 215, 1–9.
- Maser, K.R. and Roddis, W.M. Principles of Thermography and Radar for Bridge Deck Assessment. *Journal of Transportation Engineering*. Sept/Oct 1990. pp.583-601.
- Mednis, A., Strazdins, G., Liepins, M., Gordjusins, A., & Selavo, L. (2010). RoadMic: Road surface monitoring using vehicular sensor networks with microphones. *Communications in Computer and Information Science*, 88, 417–429. doi:10.1007/978-3-642-14306-9\_42
- Melville, B. W. & Coleman, S. E. 2000 Bridge Scour. Water Resources, LLC, CO, USA,
- Miller, J.S. and Bellinger, W.Y. (2014) Distress Identification Manual for the Long-term Pavement Performance Program, 5<sup>th</sup> edition, U.S. Department of Transportation, Federal Highway Administration, Washington DC (2014)
- Milillo, P., Giardina, G. Perissin, D. Milillo, G. Coletta, A. and Terranova, C. (2019) Pre-Collapse Space Geodetic Observations of Critical Infrastructure: The Morandi Bridge, Genoa, Italy, *Remote Sensing*. Volume.11, 1403; doi:10.3390/rs11121403w
- Mondal S.K., Sastry R.G., Pachauri A.K. and Gautam P.K. 2008. High resolution 2D electrical resistivity tomography to characterize active Naitwar Bazar landslide, Garhwal Himalaya, India. *Current Science* 94, 871–875.

- McRobbie S., Lodge R., and Wright A., 2007, automated inspection of highway structures – Stage 2, PPR 255, Transportation Research Laboratory, UK.
- MDOT (2009) Minnesota Department of Transport, Bridge Health Monitoring and Inspections Systems - A Survey of Methods, Downloaded from www.
- Murphy, R., Steimle, E., Hall, M., Lindemuth, M., Trejo, D., Hurlebaus, S., Medina-Cetina, Z., (2011) Robot-assisted bridge inspection. *Journal of Intelligent Robot Systems*, 64(1), 77–95
- Nassif, H., Ertekin, A. O., & Davis, J. (2002). Evaluation of bridge scour monitoring methods. United States Department of Transportation, Federal Highway Administration, Trenton.
- Nazarian S. and Stokoe K.H. 1984. In situ shear wave velocities from spectral analysis of surface waves. *Proceedings of the 8th World Conference on Earthquake Engineering*, San Francisco, California, USA, Expanded Abstracts, 31–38.
- NPRA (2005) Norwegian Public Road Administration, Handbook for Bridge Inspections
- Oats, R.; Escobar-Wolf, R.; Oommen, T. A Novel Application of Photogrammetry for Retaining Wall, Assessment. *Int. Journal. Infrastructures* 2017, 2, 10.
- Overmeeren, R. A., S. V. Sariowan, and J. C. Gehrels (1997). Ground Penetrating radar for determining volumetric soil water content; results of comparative measurements at two test sites., v. 197, p. 316-338.
- Plati, C., and Loizos, A. (2013) Estimation of in-situ density and moisture content in HMA pavements based on GPRtrace reflection amplitude using different frequencies. *J. Appl. Geophys.* Vol 97, pp 3–10.
- Plati, C., A. Loizos, and K. Gkyrtis, (2020) Integration of non-destructive testing methods to assess asphalt pavement thickness: *NDT & E International*, v. 115.
- Prendergast, L. J. and Gavin. K. (2014). A review of bridge scour monitoring techniques. *Journal of Rock Mechanics and Geotechnical Engineering*, 6(2), 138-149
- Prendergast, L. J., Hester, D. Gavin, K. and O’Sullivan, J. 2013. An investigation of the changes in the natural frequency of a pile affected by scour. *Journal of Sound and Vibration*, 332(25), 6685-6702
- Prendergast, L. J., Hester, D and Gavin, K. (2016b). Determining the presence of scour around bridge foundations using vehicle-induced vibrations. *Journal of Bridge Engineering*, Article ID 04016065.746
- Prendergast, L. J., Hester, D and Gavin, K. (2016b). Development of a vehicle-bridge-soil dynamic interaction model for scour damage modelling. *Shock and Vibration*. DOI: 74810.1155/2016/7871089
- RAIU (Railway Accident Investigation Unit). 2010. Malahide Viaduct Collapse on the Dublin to Belfast Line, on the 21st August 2009. InvestigationRep.No.2010-R004.Blackrock,Ireland
- Park,B. J.Kim,J.Lee,M.-S.Kang,andY.-K.An. (2018) Underground object classification for urban roads using instantaneous phase analysis of ground-penetrating radar (GPR) data,"*RemoteSensing*,Vol.10,No.9,
- Park C.B., Miller D.M. and Xia J. 1999. Multichannel Analysis of sur-face waves. *Geophysics*64, 800–808.

- Phares, B. M., Washer, G. A., Rolander, D. D., Graybeal, B.A. & Moore, M. (2004), Routine highway bridge inspection condition documentation accuracy and reliability, *Journal of Bridge Engineering*, 9(4), 403–13.
- Popescu, C., Tajsten, B. Blanksvard, T. and Elfgrén, L. (2019) 3D reconstruction of existing concrete bridges using optical methods, *Structures and Infrastructure Engineering*. Vol. 15, No. 7, pp. 912–924.
- Prendergast, L. J., Hester, D., Gavin, K., & O'Sullivan, J. J. (2013). An investigation of the changes in the natural frequency of a pile affected by scour. *Journal of Sound and Vibration*, 332(25), 6685-6702.
- Puente, I.; González-Jorge, H.; Riveiro, B.; Arias, P. (2013) Accuracy verification of the Lynx Mobile Mapper system. *Opt. Laser Technol.*, 45, pp. 578–586.
- Ragnoli, A.; De Blasiis, M.R.; Di Benedetto, A. Pavement distress detection methods: A review. *Infrastructures*, 2018, Vol 3, No. 58.
- Sansalone, M.J. (1993), "Detecting delaminations in concrete bridge decks with and without asphalt overlays using an automated impact-echo field system", *NDT in Civil Engineering*, Proceedings of the Intl. Conference of British Institute of Non-Destructive Testing, Liverpool, U.K., April 14-16.
- Sansalone, M. J., and W. B. Streett, 1998, *The Impact-Echo Method: NDTnet*, v. 3.
- Safi, M., Sundquist, H. Karoumi, R and Racutanu, G. (2013) Development of the Swedish bridge management system by upgrading and expanding the use of LCC, *Journal of Maintenance, Management, Life-Cycle Design and Performance*, Volume 9, 2013 - Issue 12
- Schmutz M., Albouy Y., Gurin R., Maquaire O., Vassal J., Schott J.-J. and Desclotres M. 2000. Joint electrical and time domain electromagnet-ism (TDEM) data inversion applied to the super sauze earthflow (France). *Surveys in Geophysics* 21, 371–390
- Shinoda, M., Haya, H. and Murata, S. (2008) Non-destructive Evaluation of Railway Bridge Substructures by Percussion Tests, 4th Int. Conf. on Scour and Erosion, Tokyo. Pp.285-290.
- Shirole, A., and R. Holt, (1991). Planning for a Comprehensive Bridge Safety Assurance Program: *Transportation Research Record* 1290.
- Spielhofer, R., Benbow, E. and Wright, A. (2015) HiSPEQ Deliverable – Identifying the key requirements for surface condition measurements – report for consultation, [www.cedr.eu](http://www.cedr.eu)
- Suzuki K. and Higashi S. 2001. Groundwater flow after heavy rain in landslide-slope area from 2-D inversion of resistivity monitoring data. *Geophysics* 66, 733–743.
- Thornes et al. (2012) *Climate Change Risk Assessment for the Transport Sector*, Dept. for Food and Rural Affairs, London, UK.
- Truong-Hong, L., and D. F. Laefer, (2014). Application of Terrestrial Laser Scanner in Bridge Inspection: Review and an Opportunity, 37th IABSE Symposium: Engineering for Progress, Nature and People., Madrid, Spain, International Association for Bridge and Structural Engineering (IABSE).
- Truong-Hong, L., Falter, H. Lennon, D. and Laefer, D. (2016) Framework for bridge inspection with laser scanning." In *Proc., 14th East Asia-Pacific Conf. on Structural Engineering and Construction (EASEC-14)*, 1–9. Ho Chi Minh City, Vietnam: EASEC.

- Wai-Lok Lai, W., Dérobert, X., Annan, P., 2017. A review of ground penetrating radar application in civil engineering: a 30-year journey from locating and testing to imaging and diagnosis. *NDT E Int*:pp. 1–22 <http://dx.doi.org/10.1016/j.ndteint.2017.04.002>
- Worley, R., Dewoolkar, Xia, T. Farrell; R. Orfeo, D. Burns,D. and Dryver R. (2019) Acoustic Emission Sensing for Crack Monitoring in Prefabricated and Pre-stressed Reinforced Concrete Bridge Girders, *Journal of Bridge Engineering*, Vol. 24, No.4.
- Wright, A., et al. (2016) Hi-SPEQ – developing the technical and quality requirements for high-speed condition surveys of road networks., *Transport Research Procedia*, VI. 14, pp 2956-2965.
- Xia J., Miller R.D. and Park C.B. 1999. Estimation of near surface shear wave velocity by inversion of Raleigh waves. *Geophysics*64, 691–700.
- Yehia, S., Abudayyeh, O., Nabulsi, S. and Abdelqader, I. “Detection of Common Defects in Concrete Bridge Decks Using Nondestructive Evaluation Techniques.” *Journal of Bridge Engineering*. Mar/Apr 2007. pp. 215-225.
- Yu, X., & Yu, X. (2009). Time domain reflectometry automatic bridge scour measurement system: principles and potentials. *Structural Health Monitoring*, 8(6), 463-476. <https://doi.org/10.1177%2F1475921709340965>
- Zarafshan, A., Iranmanesh, A., & Ansari, F. (2011). Vibration-based method and sensor for monitoring of bridge scour. *Journal of bridge engineering*, 17(6), 829-838. [https://doi.org/10.1061/\(ASCE\)BE.1943-5592.0000362](https://doi.org/10.1061/(ASCE)BE.1943-5592.0000362)
- Zhang, Y., Mcdaniel, J. G., & Wang, M. L. (2013). Estimation of pavement macrotexture by principal component analysis of acoustic measurements. *Journal of Transportation Engineering*, 140(1), 1–12. doi: